https://doi.org/10.17113/ftb.62.02.24.8162 original scientific paper

In silico, *In vitro* and *Ex vivo* Evaluation of the Antihyperglycaemic, Antioxidant and Cytotoxic Properties of *Coccinia grandis* L. Leaf Extract

Running Title: Extraction and Identification of Bioactive Phytocompounds for Food and Health

Pawan Prabhakar[1], Sayan Mukherjee[2], Ankit Kumar[3], Rahul Kumar Rout[3], Suraj Kumar[1], Deepak Kumar Verma[3], Santanu Dhara[2], Pavuluri Srinivasa Rao[3], Mrinal Kumar Maiti[4] and Mamoni Banerjee[1]*

[1]Bio-Research Laboratory, Rajendra Mishra School of Engineering Entrepreneurship, Indian Institute of Technology Kharagpur, Kharagpur 721 302, West Bengal, India
[2]School of Medical Science and Technology, Indian Institute of Technology Kharagpur, Kharagpur 721 302, West Bengal, India
[3]Agricultural and Food Engineering Department, Indian Institute of Technology Kharagpur, Kharagpur 721 302, West Bengal, India
[4]Department of Biotechnology, Indian Institute of Technology Kharagpur, Kharagpur 721 302, West Bengal, India

Received: 21 March 2023
Accepted: 13 May 2024

SUMMARY

Research background. Coccinia grandis (L.) is traditionally used for the management of diabetes mellitus. Since, scientific evidence and the mechanism of action have yet to be investigated extensively, this study aimed to evaluate the antidiabetic and cytotoxic effects together with the optimization and development of a scale-up process design for higher yields of bioactive phytocompounds from *C. grandis.*

*Corresponding author:
Phone: +919968681611
E-mail: mamoni@see.iitkgp.ac.in

Experimental approach. The *in silico* study was performed to predict the binding affinity of phytocompounds of *C. grandis* for α-amylase and α-glucosidase enzymes involved in the pathophysiology of diabetes with pharmacokinetic assessment. Response surface methodology was employed to determine the optimum values for TPC, TFC, TTC and antioxidant activities (DPPH and FRAP) across 17 separate experimental runs that varied microwave-assisted extraction parameters like temperature (50–70 °C), power (400–1000 W) and time (15-45 min). The purification and identification phytocompounds were done by column chromatography, TLC, UV-Visible, FTIR and LC-MS spectral analysis, respectively. The *in vitro* antidiabetic activity was done by α-amylase and α-glucosidase enzymatic inhibitory assay while cytotoxic investigations were done by percentage hemolytic activity, MTT and CAM assay.

Results and conclusions. The reported major bioactive compounds have demonstrated an excellent binding affinity for α-amylase and α-glucosidase enzymes in the range of −3.7 to −8.6 kcal/mol with good pharmacokinetic properties and toxicities ranging from low to medium. The bioactive constituents such as TPC, TFC, TTC and antioxidant activities like DPPH and FRAP were found to be high and depend on the microwave-assisted optimized extraction parameters like temperature, time and power: 55 °C, 45 min, and 763 W, respectively. Sixteen compounds were identified by their FTIR and LC-MS spectra in the plant sample after preliminary identification, purification and TLC. The percentage enzyme inhibition was dependent on the concentration of the extract (7.81–125 μg/mL), and was found to be higher than acarbose. The hemolytic activity was found to be compatible with ISO standards and in MTT and CAM assay, low toxicity was observed in the range 7.81−125 μg/mL, which supports its potential use as antidiabetic drug formulation as well as functional food development.

Novelty and scientific contribution. Researchers, scientists, and businesspeople in the food and pharmaceutical sectors will have new opportunities due to the study's findings to develop antidiabetic food formulations and medications to help diabetics for better control their condition and maintain overall health.

Keywords: diabetes mellitus; *Coccinia grandis*; phytochemicals; optimization; molecular docking; enzyme inhibition; cytotoxicity

INTRODUCTION

Diabetes mellitus, a prevalent medical condition, encompasses a collection of enduring metabolic disorders distinguished by the presence of hyperglycemia, or elevated levels of glucose in the bloodstream. The symptoms above manifest as a result of compromised insulin secretion, insulin action, or a combination of both (*1*). Prolonged elevation of blood glucose levels can lead to severe detrimental effects on various physiological systems, such as renal dysfunction, myocardial infarction, cerebrovascular accidents, retinal damage, and the formation of opacities in the lens of the eye (*2*). The global prevalence of diabetes is experiencing an upward trend, leading to an increasing number of individuals affected by this metabolic disorder worldwide. Based on the projections provided by the International Diabetes Federation (IDF), it is estimated that the global population of individuals affected by diabetes, both diagnosed and undiagnosed, will reach approximately 536.6 million in the year 2021. Furthermore, it is anticipated that this figure will experience a substantial increase of 46 % over the course of the next 24 years, reaching a staggering 783.2 million by the year 2045 (*3*). The enzyme inhibitors drug such as acarbose, miglitol, and voglibose are the ones that are being used for the purpose of postprandial hyperglycemia (PPHG) management. However, both miglitol and voglibose exclusively inhibit α-glucosidase, but acarbose is effective in inhibiting both α-amylase and α-glucosidase (*4*). Because of the adverse effects on the gastrointestinal tract that these inhibitors might cause, long-term medication is not recommended. Drugs from natural origins have enormous benefits in treating chronic disorders with fewer or no side effects. They are compatible with human physiology and wide acceptability among common people (*5,6*). Therefore, researchers are focusing on both α-amylase and α-glucosidase inhibitors drugs having natural in origin like plants, microbes, marine etc.

The leaves and fruits of *Coccinia grandis* (L.) are utilized as ethnomedicinal agents and dietary components for the management of diabetes within diverse tribal populations. Despite the widely recognized physiological impact of *C. grandis* and its involvement in various health and disease processes, there has been a notable scarcity of research efforts dedicated to the formulation of therapeutic interventions utilizing the phytoconstituents derived from this botanical species. Prior studies have demonstrated the potential advantages of employing *C. grandis* leaf extract for the purpose of diabetes management *(7)*. Nevertheless, there is a need for more scientific literature available that can

provide a comprehensive understanding of the exact mechanism underlying the antidiabetic effects and toxicity assessment.

Given the afore mentioned circumstances, the objective of the current research was *in silico*, *in vitro*, and *ex vivo* to examine the potential of the phytocomponents of *C. grandis* in treating diabetes. This was achieved by studying their ability to inhibit the enzymes α-amylase and α-glucosidase, as well as by conducting investigations on the drug's absorption, distribution, metabolism, and excretion (pharmacokinetics) and its potential to cause harm to cells (cytotoxicity). The overarching goal of is to broaden the breadth of academic, scientific, and industrial efforts related to the development of antidiabetic foods and drugs as well as their formulations.

MATERIALS AND METHODS

In silico analysis

The software utilized in this study includes AutoDock Tools, developed by The Scripps Research Institute in the United States (*8*), Discovery Visual 2020 software, developed by Dassault Systemes in France (*9*), and Open Babel, specifically the Open Babel GUI, Version 2.4.1 (*10*). The online web server employed in this study was Admetlab 2.0 (*11*).

Chemicals and reagents

Ethanol (99.9 % purity), methanol (99 % purity), sodium carbonate (99 % purity), aluminium chloride (99 % purity), hydrochloric acid (HCl, 37 % concentration), ferric chloride (99 % purity), and sodium phosphate (96 % purity) were procured from Merck, Mumbai, Maharashtra, India. The Folin-Ciocalteu reagent (98 % purity) and the 3-[4,5-dimethylthiazol-2-yl]-2,5-diphenyl tetrazolium bromide (MTT) assay (98 % purity) were acquired from HiMedia, Thane, Maharashtra, India. Highly purified standards, namely quercetin (with a purity of 95 %), stigmasterol (with a purity of 95 %), and kaempferol (with a purity of 95 %), were procured from Sigma Lifesciences, Bangluru, Karnataka, India. Silica gel with a mesh size of 60-120 and a thin-layer chromatography (TLC) plate with an F254 coating were acquired from Merck, Darmstadt, Hesse, Germany. Trolox (97 % purity) and soy lecithin (95 % purity) were obtained from Sigma-Aldrich, Bangaluru, Karnataka, India. Gallic acid (99 %), tannic acid (98 %), trolox (97 %), 2,4,6-tripyridyl-*S*-triazine (TPTZ, 99 %), porcine pancreatic α-amylase, α-glucosidase, dimethyl sulfoxide (DMSO, 99 %), acarbose (95 %), starch solution, 3,5-dinitrosalicylic acid (DNSA, 99

%), and *p*-nitrophenyl-β-D-galactopyranoside (*p*-NPG, 99 %) were procured from SRL Chemicals, Mumbai, Maharashtra, India. Culture media such as Dulbecco's Modified Eagle Medium (DMEM) were procured from Gibco, Life Technologies Ltd., Paisly, UK, along with other reagents of analytical grade.

Molecular docking studies

Based on prior scientific investigations and comprehensive databases, 19 prominent bioactive phytocompounds exhibiting both antidiabetic and antioxidant characteristics have been successfully identified. The acarbose compound, a commonly used therapeutic agent, was acquired from PubChem (*12)* in sdf format and subsequently transformed into the pdb format using Open Babel software (*10*). The utilization of Lipinski's rule of five in this context was facilitated by the advanced computational resources accessible at the bioinformatics and computational biology supercomputing facilities of the IIT Delhi. The crystal structures of the α-amylase and α-glucosidase enzymes were deposited into the protein data bank by Tan *et al.* (*13*) and Lodge *et al.* (*14*) at resolutions of 1.35 *Å* and 1.90 *Å*, respectively and used in the analysis. Discovery Studio (*9*) was employed for the removal of water molecules, heteroatoms, and ligands. AutoDock (*8*) was utilized to introduce gastgeiger charges to the central grid. The central grid was configured to rejuvenate the active site pockets. The values for the center grids and the total number of points are provided in Table S1. To achieve maximum accuracy in docking procedures, we maintained the exhaustiveness level at 100. Initially, a molecular docking procedure was employed to investigate the interaction between acarbose and enzymes. Subsequently, phytochemical compounds were introduced into the system. AutoDock Vina executed the docking process utilizing its command mode, while Discovery Studio facilitated the visualization of the molecular structure.

Pharmacokinetic analysis

The pharmacokinetic analysis resulted into different values of absorption, distribution, metabolism, excretion and toxicity.

Optimization of MAE parameters

Leaf samples were procured and collected from plants of the agricultural land belonging to the Agriculture and Food Engineering Department, Indian Institute of Technology Kharagpur, located in Kharagpur, India, at coordinates 22.31 °N and 87.31 °E. After the authentication, the leaves were washed, air-dried for 45 days, sealed and preserved. Based on prior scientific investigations, it has been

determined that ethanol with a concentration of 80 % and the utilization of microwave-assisted extraction (MAE) represent the most effective solvents and extraction methodologies for the retrieving phytocompounds, such as polyphenols. The extraction efficiency during the MAE process can be influenced by temperature, time, power and other factors to maximize the production of desired outcomes.

Experimental design

As per the study conducted by Dahmoune *et al.* (*15*), the optimizing extraction variables utilized a three-level Box Behnken Design (BBD) comprising three factors. The independent variables in the study were temperature, power and time, specifically ranging from 50–70 °C, 400–100 W, and 15 to 45 min, respectively. Preliminary experiments and prior research have established the limits of the variables involved. The solvent-to-sample ratio was determined to be 8:1 and ethanol (80%) was used as solvent. The total phenolic content (TPC), total flavonoid content (TFC), total tannin content (TTC), 2,2-diphenyl-1-picrylhydrazyl (DPPH), and ferric reducing antioxidant power (FRAP) were measured as the antioxidant capacities of the plant extracts. This study employed Design Expert software (Version 11.12.0) and the BBD with five central points (*16*). The response variables were modeled using a second-order polynomial equation (Eq. 1).

$$Yi = \beta_0 + \beta_1 x_1 + \beta_2 x_2 + \beta_3 x_3 + \beta_{11} x_1^2 + \beta_{22} x_2^2 + \beta_{33} x_3^2 + \beta_{12} x_1 x_2 + \beta_{23} x_2 x_3 + \beta_{13} x_1 x_3 \quad /1/$$

where Yi represents the response variable; β_0 denote the constant term, β_1, β_2, and β_3 represent the regression coefficients for the linear terms; β_{11}, β_{22}, and β_{33} represent the regression coefficients for the quadratic terms, while β_{12}, β_{23}, and β_{13} represent the regression coefficients for the interaction terms. The independent variables, x_1, x_2, and x_3, correspond to temperature, power, and time, respectively. Three experimental runs were conducted, and the mean values were analyzed. The model's appropriateness was verified based on R^2 value, p-value, CV-value, and lack of fit.

Determination of phytocompound contents

Total phenol content

The determination of the TPC in the leaf extract of *C. grandis* was conducted using the methodology proposed by Do *et al.* (*17*), with certain adjustments. The extracts of plant were collected

and gallic acid solutions with varying concentrations (100-500 μg/mL) were prepared. These solutions were then used to create a calibration curve based on a linear equation. Once more, a volume of 0.5 mL of crude extracts possessing a concentration of 0.1 mg/mL was introduced into a test tube. Subsequently, 0.5 mL of distilled water and 1 mL of the Folin-Ciocalteu reagent were mixed. Following a time interval of 3 min, a volume of 2 mL of sodium carbonate solution with a concentration of 20 % w/V was introduced into the mixture. Subsequently, the mixture was placed in dark at a temperature of 25 °C for a duration of 60 min. The absorbance of the sample was subsequently measured at 765 nm by comparing it to a blank using a ultraviolet-visible (UV-Vis) spectrophotometer (SHIMADZU UV 1601, Kyoto, Kansai, Japan). Upon conducting an examination of the calibration curve, the TPC of the plant was determined and expressed as mgGAE/g DM. The experiment was conducted in triplicate (N=3), and the means were calculated along with their corresponding standard deviations.

Total flavonoid content

The TFC w*a*s determined using the aluminium chloride colorimetric method, following the protocol proposed by Sen *et al.* (*18*), with minor modifications. Initially, a total volume of 3 mL of distilled water was combined with 1 mL of each respective extract sample. Once more, a volume of 0.2 mL of aluminium chloride solution with a concentration of 10 % was introduced into the mixture. Following a 10 min incubation period, a solution containing 0.2 mL of potassium acetate with a concentration of 1M was introduced into the mixture. Subsequently, 6 mL of distilled water was added to achieve the desired final volume. The solution was allowed to undergo a period of undisturbed incubation for a duration of 30 min. Following this, it was subjected to analysis utilizing a UV-Vis spectrophotometer (SHIMADZU UV 1601, Kyoto, Kansai, Japan) to ascertain its absorbance at a wavelength of 415 nm. The quercetin concentrations (50-500 μg/mL) were prepared and utilized to generate a standard calibration curve. The measurement of the outcomes was expressed in milligrams of quercetin equivalent per gram of dry mass (mgQE/g DM). The experiment was conducted in triplicate (N = 3), and the means were calculated along with their corresponding standard deviations.

Total tannin content

The technique for assessing the TTC was established by Kumar *et al.* (*16*), incorporating certain adjustments as necessary. Initially, a volume of 1 mL of the diluted extracts was introduced into a solution

containing 0.5 mL of the Folin-Ciocalteu reagent. This mixture was subsequently allowed to remain undisturbed for a duration of 3 min. Again a volume of 1 mL of sodium carbonate (7.5 % concentration) was introduced into the amalgamation and allowed to undergo a 30 min incubation period at a temperature of 25 °C in dark. Tannic acid was employed as the reference standard, and the standard calibration curve was derived by employing a concentration range of 100–500 µg/mL. The measurement of absorbance was conducted using a UV-Vis spectrophotometer (SHIMADZU UV 1601, Kyoto, Kansai, Japan). The spectrophotometer was set to a fixed wavelength of 593 nm, and the data was collected meticulously. The regression analysis employed the calibration curve to determine the concentration of tannic acid equivalent in milligrams per gram of dry mass (mgTAE/g DM). The experiment was conducted in triplicate (N = 3), and the means were calculated along with their corresponding standard deviations.

Determination of antioxidant activities

DPPH antioxidant activity

The methodology stated by Marinova and Batchvarov (*19*) with certain changes was employed to determine the DPPH antioxidant activity of the solvent extract from *C. grandis*. A volume of 1 mL of plant extract was subjected to dilution by combining it with 2 mL of methanol in a test tube. Briefly, a volume of 1 mL of DPPH-methanol solution with a concentration of 0.004 mM was introduced to a volume of 3 mL of plant extracts. The mixture was then subjected to 30 min incubation in dark. Absorbance at a wavelength of 517 nm was measured using a UV-Vis spectrophotometer (SHIMADZU UV 1601, Kyoto, Kansai, Japan). The radical scavenging capacity of the sample was determined by applying the percentage radical activity formula, denoted as Eq. 2. The experiment was conducted in triplicate (N = 3), and the means were calculated along with their corresponding standard deviations.

$$\text{Radical scavenging activity (\%)} = [(A_{Control} - A_{Sample}/A_{Control}) \times 100] \quad /2/$$

FRAP antioxidant activity

The experiment was conducted to measure the reducing antioxidant power using the protocols outlined by Benzie and Strain (*20*), with minor modifications. The FRAP reagent was prepared by combining 150 mL of acetate buffer, 5 mM of TPTZ dissolved in 20 mM of HCl and 10 mM of Ferric chloride hexahydrate ($FeCl_3.6H_2O$) in a 10:1:10 ratio. Following the addition of 1 mL of a freshly prepared

reagent to 2 mL of each of the diluted plant extracts, the mixture was thoroughly homogenized. Subsequently, the mixture was incubated at a temperature of 37 °*C* for a duration of 30 min. The resulting outcome exhibited an exceptionally vibrant blue color. To determine this, the absorbance at a wavelength of 593 nm was measured using a UV-Vis spectrophotometer (SHIMADZU UV 1601, Kyoto, Kansai, Japan). A reagent blank was employed as a reference, consisting of 2 mL of FRAP reagent and 1 mL of deionized (DI) water. After conducting the experiment involving the construction of a calibration curve using Trolox at concentrations ranging from 1 to 5 mg/mL, which successfully determined the concentrations of the antioxidant standard. The concentration of FRAP to determine the extent of antioxidant activity was expressed as milligrams of Trolox equivalent per gram of dry mass of the plant sample (mgTE/g DM). The experiment was conducted in triplicate (*N*=3), and the means were calculated along with their corresponding standard deviations.

Preliminary phytochemical screening, purification, and thin layer chromatography of plant extract

The phytochemical screening of bioactive compounds in plant extracts using appropriate reagents is one of the preliminary detection methods for primary and secondary metabolites. Previous studies have confirmed the use of established methods for evaluating the phytochemical composition of plant leaf extracts (*21-23*). These methods were employed to conduct initial screenings of phytocompounds. Utilizing slight adjustments, column chromatography was employed for the analysis of the unprocessed leaf extracts, as reported by Chandrappa *et al.* (*24*). A slurry was prepared by combining silica gel with a mesh size ranging from 230 to 400 with *n*-hexane. Again the silica gel was densely packed with a slurry to prevent any subsidence. The column was primed with an empty run and subsequently flushed with *n*-hexane to optimize the solvent flow rate within the column. A conical flask was placed at the base of the column, in close proximity to its terminal point, to collect the eluate. The material that was obtained was subsequently deposited onto the column, and the selection of the mobile phase was carried out using thin TLC with the specified combination of solvents. Toluene, ethyl acetate, methanol, and formic acid in a ratio of 75:25:25:6 were employed as solvents in the experiment. The migration of the desired compound was monitored using a silica gel plate. A total of seven fractions were obtained following the implementation of an isocratic mobile phase consisting of toluene, ethyl acetate, methanol, and formic acid in the ratios of 200:64:64:16. Each segment possesses a volumetric capacity of 56 mL. The aliquots were collected, concentrated utilizing a rotary evaporator, and subsequently subjected to TLC analysis.

The chromatographic separation employed a mobile phase consisting of toluene, ethyl acetate, methanol, and formic acid in a ratio of 5:1.6:1.6:0.4. The resulting spots were then compared to reference standards of quercetin and kaempferol. Fraction 2 and Fraction 3 were mixed, and the resulting mixture was subsequently subjected to a repetition of column chromatography for the purpose of comparison with quercetin and kaempferol standards.

Identification and characterization of bioactive phytocompounds

UV-visible spectrophotometer

This study was conducted to analyze the UV-Vis spectrum of the plant extract. The investigation utilized a wavelength range spanning from 200 to 700 nm, following the methodology proposed by Sharma *et al.* (*25*). The reference compounds, pure standard quercetin and kaempferol, were utilized for their respective spectra. The spectra were obtained using a quartz cuvette with a path length of 10 mm, employing a UV-Vis spectrophotometer (SHIMADZU UV 1601, Kyoto, Kansai, Japan).

Fourier transform infrared spectral study

The identification of functional groups and their corresponding vibrating frequencies in the leaf extract was performed using Fourier transform infrared spectroscopy (FTIR) (Nicolet 6700 spectrophotometer, Thermo Fisher Scientific, Waltham, Massachusetts, USA). The active functional groups of the components were classified into different categories according to their respective peak frequencies (*26*). As per the findings of Patle *et al.* (*27*), the vibrational frequency of functional groups is considered to be the distinctive “fingerprint” of an organic molecule. The sample was mixed with potassium bromide and analyzed using FTIR. The observed absorbance band in the FTIR spectra of *C. grandis* was found to correspond to wavenumbers ranging from 3500 to 400 cm^{-1}.

Liquid chromatography and mass-spectrometry of plant extract

The liquid chromatography and mass spectrometry (LC-MS) analysis of the *C. grandis* extract was conducted using the protocols described by Al-Madhagy *et al.* (*28*), with minor adjustments. Following a dilution of the extract by a 100-fold factor, the samples underwent analysis using a LC-MS system (Waters, Milford, Massachusetts, USA). The LC-MS system was equipped with a photodiode array detector operating at a wavelength of 250 nm. The analytical C18 column (Waters, Milford,

Massachusetts, USA) was employed as the stationary phase. The apparatus comprises a combined integrated and automated fraction collector. The Quattro micro™ Application Programming Interface (API) in conjunction with the upgraded mass-Lynx 4.7 software was utilized to control the instrument and acquire the data. A mobile phase comprising of an aqueous solution containing 0.1 % formic acid (A) and methanol acidified with 0.1 % formic acid (B) was employed at a flow rate of 0.5 mL/min to perform gradient elution. The gradient elution commenced with a mixture consisting of 90 % solvent A and 10 % solvent B, which was maintained from 0 to 45 min. Subsequently, the composition was transitioned to 100 % solvent B from 45 to 55 min. Following this, the eluent was reverted to a mixture of 90 % solvent A and 10 % solvent B from 55 to 55.5 min, and this composition was maintained until 60 min. Mass spectra were acquired within the mass-to-charge ratio (*m/z*) range of 50-2000 using a temperature of 400 °C and a nebulizing gas flow rate of 10 L/min. Both negative and positive ionization modes were employed and a chromatogram was recorded at a wavelength of 350 nm.

Determination of in vitro enzyme inhibitory potential

Inhibition of α-amylase enzyme

The enzyme inhibitory assay methods employed by Nair *et al.* (*29*), with slight modifications, were utilized to assess the α-amylase inhibitory activity of a plant extract. Utilizing a 5 % DMSO solution, two test tubes were prepared. In one test tube, 1 mL of plant extract was combined with 1 mL of acarbose. In the other test tube, 1 mL of 20 mM sodium phosphate buffer (pH 6.8) containing 40 µL of porcine pancreatic amylase (0.5 mg/mL) was added. The plant extract and acarbose mixture were then added to the second test tube at various doses ranging from 7.81 to 125 µg/mL. Following a period of 15 min at 25 °C, 0.5 % (w/V) starch solution was introduced into the solution. The resulting mixture was then subjected to another 20 min incubation period. Once more, a volume of 1.0 mL of DNSA solution was introduced to terminate the ongoing chemical reaction. Subsequently, the test tubes were immersed in a temperature-controlled water bath for a duration of 5 min, followed by a cooling period. Afterward, 5 mL aliquot of distilled water was added to each test tube to achieve dilution. The absorbance measurements of the samples were recorded at a wavelength of 540 nm using a UV-Vis spectrophotometer (SHIMADZU UV 1601, Kyoto, Kansai, Japan). The control solution comprises starch, enzyme, DMSO, and DNSA, while starch was utilized in the preparation of the blank. Acarbose was employed as a reference

compound, and the percentage of inhibition of the α-amylase enzyme by the plant extract was assessed using the formula for calculating percentage inhibition (Eq. 3). The experiment was conducted in triplicate (n = 3) and the means were calculated along with their corresponding standard deviations.

$$\text{Inhibition (\%)} = [(A_{Control} - A_{Sample}/A_{Control}) \times 100] \quad /3/$$

Inhibition of α-glucosidase enzyme

In separate test tubes, a volume of 1 mL of plant extract and acarbose was diluted in a 5 % DMSO solution at different concentrations ranging from 7.81 to 125 μg/mL. The methodology employed to assess the inhibitory activity of the α-glucosidase enzyme was based on the approach described by Alqahtani *et al.* (*30*), with slight modifications. A solution containing 1 mL of α-glucosidase (1 mg/100 mL) in 100 mM phosphate buffer (pH 6.8) was introduced to both the extracts and the acarbose. The resulting mixture was incubated for 15 min at a temperature of 37 °C. Subsequently, the chemical process was stopped by introducing 2.5 mL of a 0.1 M sodium carbonate solution to a mixture containing 500 μL of a 5 mM p-NPG compound, which had been previously dissolved in a 100 mM phosphate buffer (pH 6.8). The reaction was subjected to an additional incubation period of 30 min at a temperature of 37 °C. To determine the absorbance of each sample, the UV-Vis spectrophotometer (SHIMADZU UV 1601, Kyoto, Kansai, Japan) was employed. The percentage inhibition was calculated using the formula stated in Eq. 3, with acarbose serving as the reference standard. The experiment was conducted in triplicate (*N* = 3) and the means were calculated along with their corresponding standard deviations.

Determination of in vitro and ex vivo toxicity

Hemocompatibility assay

The *in vitro* hemocompatibility tests assess the impact of medical devices or substances that come into contact with blood or its components. The employed methodology was proposed by Sulaiman *et al.* (*31*) with minor adjustments. Vacutainers containing a mixture of sodium citrate and heparin sodium in a ratio of 1:9 were used to collect 5 mL of fresh human blood from a healthy individual. After subjecting the sample to centrifugation for a duration of 15 min using the centrifuge (Eppendorf 5418, Hamburg, Germany), at a speed of 4000 rpm, the resulting pallet was found to consist predominantly of red blood cells. This process was employed to effectively separate the plasma from the sample. Phosphate-

buffered saline (PBS) was employed for the purpose of rinsing and diluting the concentrated red blood cell (RBC) suspension. A volume of 200 µL of sample extract was introduced into 800 µL of PBS-RBC suspensions for the purpose of conducting tests. Positive and negative controls were established by combining 0.2 mL of diluted blood with 0.8 mL of DI water and PBS, respectively. Following a 3-h incubation period at 37 °C, all tubes underwent centrifugation using the centrifuge (Eppendorf 5418, Hamburg, Germany). The centrifugation was carried out at a speed of 5000 rpm for a duration of 10 min. A UV-Vis spectrophotometer (SHIMADZU UV 1601, Kyoto, Kansai, Japan) was used to measure the absorbance of the supernatant at a wavelength of 545 nm. This measurement was employed to determine the percentage of hemolysis using a prescribed formula denoted as Eq. 4. The experiment was conducted in triplicate (N = 3), and the means were calculated along with their corresponding standard deviations.

$$\%\,\text{Hemolysis} = {(A_t - A_{Nc})}\Big/{(A_{Pc} - A_{Nc})} \times 100 \qquad /4/$$

where A_t is the absorbance of test samples, A_{Pc} is the absorbance of positive controls, and A_{Nc} is the absorbance of negative controls.

Cell viability assay

The MTT assay was employed to evaluate the cytotoxicity of sample materials and determine the cellular viability. The methodologies were adapted based on the research conducted by Liu and Nair (*32*). Rabbit corneal L929 fibroblast cells were seeded at 4000 per well in tissue culture 96-well plates at 37 °C. No cells were seeded into blank wells. After 24 hours, *C. grandis* extract was added to the media at varying concentrations (7.81-125 µg/mL) in three separate instances. After 4 h at 37 °C, cells were washed with PBS. After 48 and 72 hours, the medium was discarded. Both the sample and control groups (cells without the sample) were then incubated in 0.5 mg/mL MTT solution. DMSO was added and stirred to dissolve the crystalline purple formazan. A microplate reader (Multiskan, Thermo Fisher Scientific, Waltham, Massachusetts, USA) measured absorbance at 595 nm. After measuring the amount of light absorbed, the cell viability percentage was determined by employing Eq. 5. The experiment was conducted in triplicate (N = 3), and the means were calculated along with their corresponding standard deviations.

Cell viability (%) = $[(A_{Sample}-A_{Blank})/ (A_{Control}-A_{Blank}) \times 100]$ /5/

Chorioallantoic membrane assay

The chorioallantoic membrane (CAM) assay is a simple and cost-effective *ex vivo* model employed for evaluating the toxicity of pharmacological samples. The toxicity assessment utilizing the chick CAM model was conducted employing the methodologies outlined by Schneider-Stock *et al*. (*33*), with necessary modifications. The fertilized chicken eggs came from a government-run poultry farm in Paschim Medinipur, India. Prior to incubation at a temperature of 37 °C and a relative humidity of 80 %, all eggs were subjected to a mild sterilization procedure involving the use of ethanol (70 %). The eggs were partitioned into six distinct experimental cohorts, which encompassed a positive control, after a duration of two days of incubation. A set of five dilutions were prepared from the original stock solution, resulting in concentrations ranging from 7.81 to 125 µg/mL. A precise aperture of approximately 1 cm^2 was formed on the eggshell, specifically on the side opposite to the rounded edge. The initial chorionic membrane was carefully excised and subjected to a wash with a phosphate buffer solution (pH 7.4). Experimental groups 1 to 5 were subjected to treatments involving the administration of extract at different concentrations ranging from 7.81 to 125 µg/mL. In contrast, the positive control group did not receive any form of treatment. The eggs were carefully sealed using paraffin tape and subjected to incubation conditions of 37 °C temperature and 80 % relative humidity. Photographs of the eggs were captured at specific time intervals of 48 and 72 h using a digital camera (Nikon D7500, Nikon Inc. Melville, New York, USA). The analysis of these photographs was conducted using Image J software v. 1.54 (*34*).

Statistical analysis

The experimental results were presented in the form of the mean and standard deviation of the triplicate measurements. The statistical analyses were conducted using SPSS software version 20.0 to perform analysis of variance (ANOVA) on the experimental data (*35*). A significant difference was observed among all results at the $p<0.05$ and $p<0.01$ significance levels, as determined by the application of Tukey's HSD post hoc tests to measure significant differences in the data (*36*).

RESULTS AND DISCUSSION

In silico studies and pharmacokinetic assessment of C. grandis phytocompounds

The binding affinities of standard acarbose towards α-amylase and α-glucosidase were determined to be −5.2 and −8.1 kcal/mol, respectively, as shown in Table 1. To predict potential interactions between the α-amylase enzyme and phytochemicals, docking procedure was performed where all 19 phytochemicals were positioned at the active site of the catalytic region of the enzyme. The outcomes of the molecular docking analysis exhibited favorable affinities for the binding of the compound to α-amylase. Quercetin exhibited a remarkable affinity due to its average bond order ranging from 2.54 to 5.0 and the highest recorded binding affinity of −7.8 kcal/mol. Enhanced inhibitory activities were observed when stronger interactions occurred, characterized by a decrease in bond order. This is primarily attributed to the presence of a larger number of Van der Waals interactions, along with the involvement of two hydrogen bonds (Asp286 and Ser294) and one pi-alkyl interaction (Trp287) (refer to Fig. S1). The phytochemical compounds derived from *C. grandis* demonstrated significant inhibitory properties and strong affinities for α-glucosidase, with binding energies ranging from −3.7 to −8.6 kcal/mol. Campesterol exhibited the most favorable binding affinity, as it was evidenced by its binding energy of −8.6 kcal/mol. It also exhibited a notable level of binding affinity across a wide range of interactions and bond orders. Limited research has been conducted on the *in silico* molecular docking investigations of *C. grandis* to elucidate its potential antidiabetic effect against enzymes such as α-amylase and α-glucosidase, which are responsible for the elevated levels of glucose in the bloodstream that led to diabetes. Begum *et al.* (*37*) reported that the phytocompounds found in *C. grandis*, such as β-amyrin acetate and β-cryptoxanthin, exhibited PPAR-γ agonistic properties and demonstrated binding affinities of −4.17 and −5.5 kcal/mol, respectively. In a study conducted by Prabhakar *et al.* (*38*), molecular docking was performed on the dipeptidyl peptidase-4 (DPP4) enzyme. The researchers discovered that derivatives of phytosterols known as stigmasterol, found in *C. grandis*, exhibited a binding affinity of −8.4 kcal/mol. Hence, molecular docking emerges as a promising approach employed in the identification of potential compounds that possess the capability to serve as primary therapeutics for the treatment of diabetes.

The pharmacokinetic analysis of the 19 reported compounds was conducted with the exception of isosteviol, luteolin, listroside, oleuropein, and quercetin, all of the phytocompounds exhibited favorable potential for absorption by human intestinal tissue, as indicated by the Caco-2 permeability prediction commonly conducted on human colon cancer cell lines (*39*). The majority of phytocompounds exhibited

limited ability to traverse the blood-brain barrier, which is a critical requirement for medications targeting peripheral systems to mitigate potential adverse effects on the central nervous system (*40*). The compound p-glycoprotein plays a key role in drug efflux, meaning it helps remove drugs from cells. Consequently, activating p-glycoprotein would lead to an elevation in drug efflux, causing lower drug concentrations than required. This could potentially lead to therapeutic failure. Compounds such as ethisterone, camptothecin, isosteviol, kaempferol, quercetin, lukianol, sinapic acid, and undecanol have been identified as having low substrate affinity for p-glycoprotein. On the other hand, benzofuranone, coniferyl alcohol, ferulic acid, furanone, methyl caffeate, and p-coumaric acid are less likely to act as inhibitors of *p*-glycoprotein, as indicated in Table S2. A variety of physiological methodologies were employed to evaluate the toxicity of medicinal phytocompounds, as described by Xiong *et al.* (*41*). These techniques encompassed the use of hERG blockers to assess cardiac safety, hepatotoxicity evaluation to examine potential liver damage, DILI (drug-induced liver injury) assessment, ames toxicity testing to determine mutagenic potential, rat oral acute toxicity studies, skin sensitization assays, carcinogenicity investigations, eye corrosion testing, eye irritation evaluations, and respiratory toxicity analysis. All of the phytocompounds exhibited a low probability of acting as hERG blockers, while those with names such as p-coumaric acid, camptothecin, bezofuranone, isosteviol and ferulic acid demonstrated a moderate to high probability of inducing hepatotoxicity and the bioactive phytocompounds exhibited varying degrees of hepatotoxicity, as evidenced by animal model experimentation. The Food and Drug Administration (FDA) has proposed that a moderate threshold should be established for determining the harmful dosage of chemicals on humans and low to moderate degree of carcinogenicity owing to their ability to disrupt cellular metabolic processes or induce DNA damage (*42*). Upon investigation, it was determined that certain phytocompounds, namely campesterol, exhibited a rapid clearance rate from the body at a rate of 15 mL/min/kg. Conversely, other phytocompounds such as quercetin, benzafurananone, luteolin, and ferulic acid demonstrated a comparatively slower clearance rate ranging between 5 and 15 mL/min/kg. It predicted that the volume distribution would be found within the intermediate range (ranging from 0.3 to 0.9), and the majority of the phytocompounds exhibited a moderate half-life encompassing clearance. The assessment of water pollution levels and ecological imbalance was conducted by utilizing the LC_{50} DM (48 h exposure to *Tetrahymena pyriformis*, 96 h exposure to *Fathead minnow*, and 48 h exposure to *Daphnia magna*) as a means of testing the chemical concentration present in the water (*43*,*44*). The

bioconcentration factor was employed as a means of evaluating the potential hazards to human health associated with the food chain. The expected concentration of phytocompounds was predicted to be relatively low, indicating that they may pose a reduced risk to aquatic ecosystems (*43*). All the compounds identified in the present study exhibited a low to moderate level of toxicity towards both biological organisms and the surrounding ecosystem, as indicated in the supplementary tables (Tables S2, S3, S4, S5 and S6).

Microwave-assisted extraction optimization and the effect of various MAE parameters on the extraction process on the recovery of phytocompounds from C. grandis

The process of MAE was conducted under varying conditions of temperature, power and time. The variation in various response variables is shown in Table 2. The data pertaining to the fitting of the model for the response variables is presented in Table 3. The results of the statistical model fitting indicated that the quadratic model provides the most accurate representation of the data. This finding was supported by a significant regression p-value ($p<0.05$), suggesting a strong relationship between the variables. Additionally, the lack of fit is deemed insignificant ($p>0.05$), indicating that the quadratic model adequately captures the underlying patterns in the data. The range of TPC was extended from 54.453 to 88.933 mgGAE/g. The maximum TPC was achieved through MAE at a temperature of 60 °C and power levels of 700 W for a duration of 30 min. The minimum value was achieved at a temperature of 60 °C and power level of 1000 W for a processing duration of 15 min.

A second-order regression model was applied to the dataset for TPC, resulting in R^2 value of 0.92. This indicates that approximately 92 % of the variability in the data can be accounted for by the model. The regression analysis revealed that the linear relationship between temperature and extraction time, as well as the quadratic relationship between temperature and power level, had a significant impact on TPC. However, none of the interaction terms were found to be statistically significant ($p<0.05$). The response surface methodology (RSM) plots illustrating the relationship between the TPC and the independent variables are presented in Fig. 1a. The RSM plots provided a clear visualization of the relationship between MAE time and temperature and the extraction of TPC. As the extraction time and temperature increased, there was a corresponding increase in TPC extraction. On the other hand, when the power level was increased, the TPC yield initially increased, reached a maximum, and then

decreased. The experimental findings demonstrated that MAE at elevated temperatures resulted in improved extractability of phenolic compounds.

The quantitative analysis of the flavonoid content in the leaf extract of *C. grandis* revealed a range of 9.786 to 22.986 mgQE/g. A quadratic regression model was applied to the dataset, resulting in an R^2 value of 0.93. This indicates a higher level of agreement between the model and the observed data, suggesting a more accurate fit of the model. The study observed a statistically significant positive relationship ($p<0.05$) between microwave power and time, indicating that increasing these factors led to an increase in the extraction of flavonoids. However, the study did not find any significant effects of other parameters on the extraction of flavonoids. The p-value for the regression analysis was determined to be highly significant ($p<0.01$), indicating strong statistical evidence in support of the relationship between the variables. Conversely, the p-value for the lack of fit analysis was found to be highly insignificant, suggesting that the model adequately fits the data. The RSM curve, depicted in Fig. 1b, demonstrates the impact of microwave power and extraction time on TFC. It reveals that as microwave power and extraction time are augmented, there is a corresponding increase in the yield of flavonoids. The observed increase in yield with longer extraction times can be attributed to an improved mass transfer mechanism, leading to enhanced extractability (*15*). The observed outcome of the experiment indicated a negative correlation between temperature and the efficiency of flavonoid extraction. This indicates the thermo-sensitivity of *C. grandis* flavonoids. The highest concentration of TTC (37.573 mg TAE/g DM) was observed when the processing temperature was set at 60 °C, the power level was 700 W, and the processing time was 30 min. Conversely, the lowest concentration of TTC (22.653 mg TAE/g DM) was obtained when the microwave power was set at 1000 W for 30 min and the processing temperature was 70 °C. The regression analysis demonstrated a higher level of model accuracy, as indicated by an R^2 value of 0.95. Additionally, the regression p-value was found to be statistically significant, suggesting a strong relationship between the variables. Furthermore, the lack of fit was determined to be insignificant, as shown in Table 3. The mathematical expression representing the model that has been adjusted to the dataset is presented in Table 4. The statistical analysis revealed that the linear relationship between extraction time and temperature exhibited a high level of significance ($p<0.01$). The quadratic coefficients were determined to have statistical significance, indicating their impact on the outcome variable. Additionally, the interaction between temperature and power level was also found to be statistically

significant, suggesting a combined effect on the outcome variable. The utilization of RSM curves provides enhanced visual representations of the impact of independent variables on the TTC. The TTC exhibited a positive correlation with both temperature and power levels. It peaked at intermediate levels before subsequently declining (see Fig. 1c).

The assessment of the antioxidant efficacy of the *C. grandis* extract was conducted under various MAE conditions, and the results are shown in Table 2. The DPPH inhibition activity exhibited a range of 57.222 % to 86.388 %, indicating the ability of the tested samples to neutralize free radicals. On the other hand, the FRAP values ranged from 59.08 to 101.991 mgTE/g DM, indicating the capacity of the samples to reduce ferric ions. The regression analysis revealed a statistically significant ($p<0.01$) linear relationship between all independent variables and DPPH activity. The quadratic relationship between microwave power and its effect, as well as the significant interaction between temperature and power, were observed. In FRAP, it was observed that the linear relationship between extraction time and temperature, as well as the quadratic relationship between microwave power and temperature, were determined to be statistically significant. The correlation between temperature and power exhibited a statistically significant negative impact ($p<0.01$), whereas the impact of power and time was found to be statistically significant ($p<0.05$). The model exhibited a high level of statistical significance, as indicated by the regression p-value. Additionally, the lack of fit was found to be non-significant, further supporting the model's suitability for assessing DPPH and FRAP antioxidant activity. The R^2 values for DPPH and FRAP antioxidant activity were determined to be 0.98 and 0.99, respectively. These high R^2 values indicate that the quadratic models provide a better fit for the data. The RSM plots can be utilized to enhance comprehension of the data, as depicted in Fig. 1d and Fig. 1e. The observed rise in temperature exhibited a general detrimental effect on the DPPH and FRAP assays. This phenomenon could be attributed to a decline in the antioxidative capacity of bioactive compounds under elevated temperature conditions (*16*). The optimized condition was determined based on a combined desirability value of 0.862. The optimal solution which produced the highest values for the desired variables, was achieved at a temperature of 55 °*C*, a microwave power level of 763 *W*, and a processing time of 45 min. This indicates that the extractability of *C. grandis* leaf is improved when using intermediate ranges of temperature and power, with a longer processing time. The optimal values of TPC, TFC, TTC, and antioxidant activities (DPPH and FRAP) were determined to be 81.871 mg GAE/g, 21.248 mg QE/g, 35.248 mg TAE/g, 85.839

%, and 102.27 mg TE/g, respectively. The outcomes were verified through the execution of experiments encompassing a range of 10 % deviation from the optimal independent solution (Table S7). The obtained response variables at the optimal solution exhibited a high level of concordance with the optimal solution of RSM. This is evidenced by the relative error falling comfortably within the 10 % threshold, thus demonstrating the effectiveness of RSM in the process of optimization.

Process of phytocompound screening to identify their presence followed by purification, identification, and characterization achieved through the utilization of chromatography and spectroscopic techniques

The compound was obtained through the isolation process from various fractions of extracts, which were then compared with the standard compound quercetin and kaempferol. Subsequently, spots were detected and identified in the UV-Vis spectrum. A total of six distinct spots were detected on the TLC plate. Among these spots, it was expected that one of them would correspond to kaempferol, as visually depicted in supplementary figure (Fig. S2c). The findings of this investigation were supported by the previous research conducted by Mohanty *et al.* (*45*).

The presence of an aromatic ring, along with other rings, within phenolic and flavonoid compounds was responsible for the manifestation of two distinct absorption spectra. The absorption peak observed at a wavelength of 285 nm signifies the π-π* transitions occurring within the aromatic system. The absorption peak observed between 300 and 600 nm corresponds to transitions occurring within a different ring structure. It is believed that the emergence of a secondary peak in the sample is attributable to the superimposition of ligand-to-metal charge transfer (LMCT) bands. Due to this attribute, the UV-Vis approach effectively identified the chromophore moieties within the isolated molecules which have been reported from diverse botanical extracts. The plant extract was subjected to qualitative UV-Vis analysis to identify and characterize compounds containing σ-bonds, π-π*-bonds, lone pairs of electrons, aromatic rings, and chromophore groups. The obtained results were compared to the UV-Vis profiles of quercetin and kaempferol. Both standards exhibit two absorption peaks within the wavelength range of 400 nm, which signifies the presence of organic chromophores and implies the existence of phenols and flavonoids in the leaf extract (Fig. S3). These observations align with the conclusions drawn in a previous study conducted by Nowak *et al.* (*46*).

The observed FTIR spectra of *C. grandis* leaves revealed the absorption frequencies and intensities associated with each band. The extract contains a significant amount of flavonoids and other phenolic compounds, most of which possess a hydroxyl group. This characteristic accounts for the observed broad absorption frequency of 3480 cm^{-1}. The presence of methoxy, methylene, and methyl functional groups induced the stretching of –CH bonds at a frequency of 2919 cm^{-1}. However, a slightly lower frequency of 2850 cm^{-1} was observed in the phytocompounds due to the existence of alkanes. The occurrence of –C=C functional groups in all the compounds resulted in the observed peak at 1625 cm^{-1}. On the other hand, the peaks at 1449 and 1301 cm^{-1} could potentially be attributed to deformations involving $–NH_3$ and $–CH_3$, as well as other compounds containing –NH and $–CH_3$ groups, respectively. In the analysis of phytocompounds, it was observed that the stretching of the C–O bond occurs at two distinct peak positions: 1216 cm^{-1}, 1170 cm^{-1}, 1076 cm^{-1}, and 1049 cm^{-1}. Additionally, the bending of the C–C bond induces vibrational peaks at 718 cm^{-1} and 532 cm^{-1}, as depicted in Fig. 2. These findings were aligned well with the findings reported by Sharma *et al.* (*25*).

During the LC-MS analysis, distinct peaks were observed at different retention times, indicating the presence of various phytochemicals. These peaks were further characterized by their corresponding mass-to-charge ratio (*m/z*) values and prominent compounds were successfully identified based on their retention time. Compounds such as benzafuranone (*m/z* = 136.36), ethisterone (*m/z* = 310.14), ferulic acid (*m/z* = 194.63), luteolin (*m/z* = 286.20), camptothecin (*m/z* = 348.70), and conifyryl alcohol (*m/z* = 180.59) were detected and characterized at specific retention times of 5.6, 11.60, 12.63, 28.04, and 30.34 min, respectively. Kaempferol (*m/z* = 286.61) (shown in Fig. 2b) and luteolin (*m/z* = 286.20), two prominent flavonoid compounds, were successfully characterized based on their retention times of 15.10 and 17.22 min, respectively. Table S8 provides a comprehensive list of compounds detected through LC-MS, along with their respective retention times and *m/z* values.

The preliminary screening, column chromatography, and TLC analyses indicated the existence of alkaloids, phenolics, and glycoside phytocompounds, with phenolics being identified as the primary constituents. The findings were additionally corroborated through UV-visible and FTIR spectroscopic analyses. These findings agreed with previous studies conducted by Prabhakar *et al.* (*36,47*). Subsequently, a total of 16 chemical compounds were detected and characterized using LC-MS. Among

these compounds, phenolic compounds such as kaempferol and luteolin were found to be present. The compounds detected through LC-MS analysis in the present study were aligned with the findings of Al-Madhagy *et al.* (*28*).

Evaluation of the inhibitory capacity of C. grandis leaf extract through in vitro assessment of α*-amylase and* α*-glucosidase enzyme inhibition*

A significant inhibitory effect was observed upon investigation of the in vitro α-amylase inhibitory capacity of the *C. grandis* leaf extract. When comparing acarbose and leaf extract, it was observed that the inhibition of α-amylase by the leaf extract increased in a linear but gradual manner as the concentration increased up to 31.25 μg/mL. Consequently, the concentration of the leaf extract exhibited an upward trend in correlation with the suppression of α-amylase enzymes. The IC_{50} value of 52.40±2.68 μg/mL, which exceeded the inhibitory concentration of the standard acarbose, was determined as the maximum inhibitory concentration (70.80±1.16 %) at a concentration of 125 μg/mL (Table S9). In a study conducted by Pulbutr *et al.* (*7*), it was observed that the aqueous leaf extract of *C. grandis* exhibited a significant inhibitory effect on the α-amylase enzyme, as evidenced by an IC_{50} value of 8.09±0.72 μg/mL. In another study, Putra *et al.* (*48*) observed that the plant sample exhibited the most potent inhibition of α-amylase activity, with the lowest half-inhibitory concentration (IC_{50} = 0.75±0.45 mg/mL). Packirisamy and Sivaprakasam (*49*), reported that the fruit extract of *C. grandis* exhibited a significant inhibitory effect on α-amylase. The maximum inhibition, reaching 62.21±3.88 %, was observed at concentrations of 250 μg/mL and IC_{50} value at 117.64±4.54 μg/mL.

The ethanolic extract of *C. grandis* exhibited no inhibitory effects up to a concentration of 15.62 μg/mL when compared to acarbose. However, as the concentration increased at each data point, observable growth was observed. The maximum level of inhibition observed was 70.89±1.6 % at a concentration of 125 μg/mL, surpassing the inhibition percentage of the reference antidiabetic drug acarbose (Fig. S4a). The IC_{50} value of the ethanolic extract of *C. grandis* leaf was determined to be 76.49±3.97 μg/mL, demonstrating a lower inhibitory effect compared to acarbose (Fig. S4b). Furthermore, the IC_{50} values were determined at a reduced concentration, surpassing the levels observed in prior investigations (*7,47*). In another study conducted by Packirisamy and Sivaprakasam (*49*), it was observed that the extract derived from *C. grandis* demonstrated inhibitory effects on α-

glucosidase at a concentration of 250 μg/mL. The maximum inhibition achieved was 67.64±2.77 %, whereas acarbose exhibited a higher inhibition rate of 87.34±4.64 %. The IC_{50} value of *C. grandis* extract was found to be 81.6±3.64 μg/mL, whereas α-glucosidase inhibitors such as acarbose exhibited a lower IC_{50} value of 44.5±2.34 μg/mL. Based on the existing literature and recent research, it can be concluded that the extract derived from *C. grandis* exhibits α-glucosidase enzymatic activities. The presence of phytoconstituents in extracts may provide a rationale for their observed capacity to inhibit enzymes *in vitro*.

Assessment of the cytotoxicity of C. grandis leaf extract via in vitro and ex vivo toxicity evaluation

Different concentrations of *C. grandis* ethanolic extract ranging from 7.81 to 125 μg/mL were administered to L929 fibroblast cells for durations of 24 and 72 h. After 24 h of incubation, it was observed that the cellular viability was significantly reduced at concentrations of 7.81 and 15.62 μg/mL. However, at a concentration of 31.25 μg/mL, the cellular viability was found to be considerably higher. As the concentration reached a value of 62.50 μg/mL, it exhibited a decrease in magnitude, and at a concentration of 125 μg/mL, it demonstrated an exceptionally low level. The plant extract exhibited the lowest cellular viability even after a duration of 72 h at a concentration of 125 μg/mL, suggesting the presence of cytotoxic stress in the specimens for concentrations exceeding 62.5 μg/mL (Fig. 3a). In the present study, it was observed that the leaf extract of *C. grandis* exhibited the lowest cytotoxicity on cell lines at concentrations of up to 62.5 μg/mL. The findings suggested that the samples exhibited cytocompatibility within a specific concentration range, but the compounds extracted from them may exhibit cytotoxicity at higher concentrations (36,*47*). In a study, Bunkrongcheap *et al.* (*50*) reported that the application of stem and leaf extracts did not exhibit any discernible impact on the differentiation process of 3T3-L1 adipocytes. The observed reduction in lipid levels at a concentration of 400 μg/mL of leaf extract and 800 μg/mL of stem extract treatments can be attributed to their cytotoxic effects, as indicated by the MTT assay results. Based on the findings from the MTT experiment, it was observed that pre-treating with *C. grandis* extract resulted in a notable decrease in the detrimental effects caused by alloxan-induced RINm5F cell lysis (*50*). In comparison to cells treated solely with alloxan, the application of the extract resulted in a significant increase in cell viability, reaching 79.45±3.68 % at a concentration of 0.50 mg/mL. To mitigate any potential adverse effects on cellular viability caused by the extract, the concentration of the extract was limited to 0.50 mg/mL, as described by Meenatchi *et al.* (*51*).

In the study conducted by Varma and Bhaskar (*52*), the researchers determined the effective concentration of the *C. grandis* extract by analyzing the dose-response curve and calculating the IC_{50} values. The researchers achieved this by using various concentrations of the extract (2, 5, 10, 20, 40, 80, 100, and 200 µg/mL). The ethyl acetate fraction obtained from *C. grandis* did not exhibit significant cytotoxic effects, as determined by the percentage of cytotoxicity relative to the reference treated with the drug.

The induction of interference with RBCs is imperative for comprehending the host's immune response following exposure to foreign substances, thereby eliciting immunogenic reactions. As illustrated in Fig. 3b, the hemocompatibility of *C. grandis* (at concentrations ranging from 7.81 to 125 µg/mL) was demonstrated, with a maximum hemolysis rate of ~3.08 %. The hemolysis assay is a valuable tool for assessing the potential correlation between cytotoxic activity and the direct disruption of the cell membrane. The plant extract has exhibited a significantly low level of hemolytic activity, measuring at 3.8 % (*53,54*). This finding provides evidence for its strong compatibility with cellular membranes and red blood cells. Zohra and Fawzia (*53*) performed hemolytic assays on a range of plant species, finding that most plants exhibited no hemolytic activities. In another investigation, Majumder *et al.* (*55*) stated that the concentration tests of *C. grandis* extract did not exhibit any hemolytic activity toward human erythrocytes. When the concentration of the crude extracts of *C. grandis* was increased from 250 µg/mL to 500 µg/mL, there were no observable alterations in the hemolytic activity on the blood erythrocyte membrane. At concentrations of 250 µg/mL and 500 µg/mL, the observed hemolytic percentages were 0.231 % and 0.452 %, respectively. The CAM experiment demonstrated that the use of the botanical extract at various concentrations ranging from 7.81 to 125 µg/mL did not exhibit any adverse effects on angiogenesis or embryonic growth in the avian model. At intervals of 0, 48, and 72 h, as depicted in Fig. 4, it was observed that the blood capillaries exhibited ongoing expansion concurrent with the thickening of the membrane walls. As the concentration of *C. grandis* leaf extract increased, there was no observable inhibition of angiogenesis in the CAM of the chicken embryo. While in animal models conducted *in vitro*, it was observed that the aqueous extracts derived from leaves did not induce any pathological morphological changes in the tissues. Furthermore, these extracts did not exhibit any detrimental effects on the proper functioning of vital organs such as the liver, kidney, or bone marrow, as shown by Sankarganesh *et al.* (*56*).

CONCLUSIONS

The α-amylase and α-glucosidase inhibitors have been shown to effectively mitigate postprandial hyperglycemia, making them valuable therapeutic drug in the treatment of diabetes. The consumption of plant-based foods that are abundant in polyphenolic and flavonoid compounds has the potential to prevent up to 90 % of diabetes cases. Notably, the leaves of *C. grandis* have been identified as a valuable source of phenolic compounds. Hence, the identification of α-amylase and α-glucosidase inhibitors derived from botanical origins represents a highly efficacious strategy for mitigating adverse reactions and alleviating financial strain. In the present investigation, we have assessed the antidiabetic and cytocompatibility phytochemicals found in the leaf extracts of *C. grandis* using *in silico*, *in vitro* and *ex vivo* approaches. The optimal conditions of 55 °C, 763 W, and 45 min significantly influenced the TPC, TFC, TTC, DPPH % inhibition, and FRAP assays, resulting in a high recovery. The study revealed that the phytocompounds derived from *C. grandis* demonstrated a notable inhibitory effect on the activity of α-amylase and α-glucosidase enzymes. This inhibition was observed to be dependent on the concentration of the phytocompounds. The results of the MTT assay demonstrated that the extracts exhibited cytocompatibility up to a concentration of 62.50 μg/mL. Moreover, the low hemolytic activity observed further indicates the elevated cellular biocompatibility of the substance. Additionally, the CAM assay revealed no signs of cytotoxicity at all the measured concentration range of plant extract. Hence, the current investigation proposes the use of *C. grandis* leaf in the development of antidiabetic drugs and functional food products as an effective therapeutic and nutraceutical approach to manage diabetes mellitus.

ACKNOWLEDGEMENTS

The authors would like to express their gratitude to the Central Instrumentation facility (CRF), Indian Institute of Technology Kharagpur in Kharagpur, India for providing the facilities for the research. The authors would also like to express their gratitude to the Government of India's Ministry of Education for awarding scholarships.

FUNDING

No Funding was received for the research work.

CONFLICT OF INTEREST

The authors declare that there are no conflicts of interest.

SUPPLEMENTARY MATERIALS

Supplementary materials are available at: www.ftb.com.hr.

AUTHORS' CONTRIBUTION

Mamoni Banerjee conceptualized the manuscript; Pawan Prabhakar developed the framework, conducted experimental work and molecular docking analysis, tabulated experimental data, and drew the illustrations; Sayan Mukherjee performed *ex vivo* analysis; Ankit Kumar was responsible for optimization; Pawan Prabhakar wrote, interpreted, corrected, and compiled literature for the manuscripts; and Sayan Mukherjee, Ankit Kumar, Rahul Kumar Rout and Suraj Kumar revised the manuscript. The final submission of the work was reviewed by Mrinal Kumar Maiti, Santanu Dhara, Pavuluri Srinivasa Rao, Mamoni Banerjee, and Deepak Kumar Verma, who made comments and revisions. All authors critically evaluated and approved the final submission version of the work.

ORCID ID

Pawan Prabhakar: https://orcid.org/0000-0002-3665-9486
Sayan Mukherjee: https://orcid.org/0000-0001-7019-9922
Ankit Kumar: https://orcid.org/0000-0002-8765-292X
Rahul Kumar Rout: https://orcid.org/0000-0001-8871-6473
Suraj Kumar: https://orcid.org/0009-0002-8586-3114
Deepak Kumar Verma: https://orcid.org/0000-0003-2351-5296
Santanu Dhara: https://orcid.org/0000-0003-4443-7610
Pavuluri Srinivasa Rao: https://orcid.org/0000-0003-3999-173X
Mrinal Kumar Maiti: https://orcid.org/0000-0001-7803-4356
Mamoni Banerjee: https://orcid.org/0000-0002-3315-2567

REFERENCES

1. American Diabetes Association. Diagnosis and classification of diabetes mellitus. Diabetes Care. 2010;33: S62-9.

https://doi.org/10.2337/dc10-S062

2. Giri B, Dey S, Das T, Sarkar M, Banerjee J, Dash SK. Chronic hyperglycemia mediated physiological alteration and metabolic distortion leads to organ dysfunction, infection, cancer progression and other pathophysiological consequences: an update on glucose toxicity. *Biomed & Pharmaco*. 2018; 107:306-28.
https://doi.org/10.1016/j.biopha.2018.07.157
3. Ogurtsova K, Guariguata L, Barengo NC, Ruiz PL, Sacre JW, Karuranga S, et al. IDF diabetes Atlas: Global estimates of undiagnosed diabetes in adults for 2021. *Dia Res clinical Prac.* 2022;183:109118.
https://doi.org/10.1016/j.diabres.2021.109118
4. Poovitha S, Parani M. In vitro and in vivo α-amylase and α-glucosidase inhibiting activities of the protein extracts from two varieties of bitter gourd (Momordica charantia L.). *BMC Comp & Alt Med.* 2016;16(1):1-8.
https://doi.org/10.1186/s12906-016-1085-1
5. Prabhakar, P., & Banerjee, M. Antidiabetic phytochemicals: a comprehensive review on opportunities and challenges in targeted therapy for herbal drug development. Int J Pharm Res.2020a;12: 1673-1696.
https://doi.org/10.31838/ijpr/2020.SP1.242
6. Patel DK, Kumar R, Laloo D, Hemalatha S. Natural medicines from plant source used for therapy of diabetes mellitus: An overview of its pharmacological aspects. A Pacific J Trop Dis.2012;2(3):239-50.
https://doi.org/10.1016/S2222-1808(12)60054-1
7. Pulbutr P, Saweeram N, Ittisan T, Intrama H, Jaruchotikamol A, Cushnie B. In vitro α-amylase and α-glucosidase inhibitory activities of Coccinia grandis aqueous leaf and stem extracts. J Biol Sci. 2017;17(2):61-8.
https://doi.org/10.3923/jbs.2017.61.68
8. AutoDock Tools, ver 1.5.7, The Scripps Research Institute, La Jolla, CA, USA; 2020. Available from http://mgltools.scripps.edu/
9. Discovery Studio Visualizer, ver21.1.0.20298, Dassault Systèmes, Paris, France; 2021. Available from https://www.3ds.com/

10. Open Babel, ver 2.0, The Open Babel Team, University of Pittsburgh, Pittsburgh, PA, USA; 2020. Available from https://www.openbabel.org

11. Admetlab 2.0., ver 2.0, Central South University Changsha, Hunan, China; 2020. Available from http://admet.scbdd.com/

12. Kim, S., Thiessen, P. A., Bolton, E. E., Chen, J., Fu, G., Gindulyte, A., ... & Bryant, S. H. (2016). PubChem substance and compound databases. Nucleic acids res.*2016*:*44*(D1): D1202-D1213. https://doi.org/10.5530/jyp.2023.15.90

13. Tan TC, Mijts BN, Swaminathan K, Patel BK, Divne C. Crystal structure of the polyextremophilic α-amylase AmyB from Halothermothrix orenii: details of a productive enzyme–substrate complex and an N domain with a role in binding raw starch. J mol Biol. 2008;378(4):852-70. https://doi.org/10.1016/j.jmb.2008.02.041

14. Lodge JA, Maier T, Liebl W, Hoffmann V, Sträter N. Crystal structure of Thermotoga maritima α-glucosidase AglA defines a new clan of NAD+-dependent glycosidases. J Biol Chem. 2003;278(21):19151-8. https://doi.org/10.1074/jbc.M211626200

15. Dahmoune F, Nayak B, Moussi K, Remini H, Madani K. Optimization of microwave-assisted extraction of polyphenols from Myrtus communis L. leaves. Food chem. 2015; 166:585-95. https://doi.org/10.1016/j.foodchem.2014.06.066

16. Kumar, A, Rout, R K, Rao, P S, & Prabhakar, P. Optimization of pulsed mode sonication and in silico molecular docking study for antioxidant properties of mandarin (Citrus reticulata Blanco) peels. J Food Process Eng.2022; e14111:1-12. https://doi.org/10.1111/jfpe.14111

17. Do QD, Angkawijaya AE, Tran-Nguyen PL, Huynh LH, Soetaredjo FE, Ismadji S, et al. Effect of extraction solvent on total phenol content, total flavonoid content, and antioxidant activity of Limnophila aromatica. J food drug anal. 2014;22(3):296-302. https://doi.org/10.1016/j.jfda.2013.11.001

18. Sen S, De B, Devanna N, Chakraborty R. Total phenolic, total flavonoid content, and antioxidant capacity of the leaves of Meyna spinosa Roxb., an Indian medicinal plant. Chin J Nat Med. 2013;11(2):149-57.

https://doi.org/10.1016/S1875-5364(13)60042-4

19. Marinova G, Batchvarov V. Evaluation of the methods for determination of the free radical scavenging activity by DPPH. Bulg J Agric Sci. 2011;17(1):11-24.
20. Benzie IF, Strain JJ. The ferric reducing ability of plasma (FRAP) as a measure of "antioxidant power": the FRAP assay. Anal. Biochem. 1996;239(1):70-6. https://doi.org/10.1006/abio.1996.0292
21. Sasidharan S, Chen Y, Saravanan D, Sundram KM, Latha LY. Extraction, isolation and characterization of bioactive compounds from plants' extracts. Afr J Tradit Complem. 2011;8(1): 1-10. https://doi.org/10.4314/ajtcam.v8i1.60483
22. Tiwari P, Kumar B, Kaur M, Kaur G, Kaur H. Phytochemical screening and extraction: a review. Int Pharma Sci. 2011;1(1):98-106.
23. Prabhakar, P, Mamoni, B. Technical Problems, Regulatory and Market Challenges in Bringing Herbal Drug into Mainstream of Modern Medicinal Practices. Res J Biotechnol.*2021; 16 (3):* 212-222.
24. Chandrappa C, Govindappa M, Anil Kumar NV, Channabasava R, Chandrasekar N, Umashankar T, Mahabaleshwara K. Identification and separation of quercetin from ethanol extract of carmona retusa by thin layer chromatography and high performance liquid chromatography with diode array detection. World J Pharm Pharma Sci. 2014;3(6):2020
25. Sharma, A., Mazumdar, B., Keshav, A. Extraction and Phytochemical Analysis of Coccinia indica Fruit Using UV-VIS and FTIR Spectroscopy. In: Rizvanov, A.A, Singh, BK, Ganasala, P, editors. Advances in Biomedical Engineering and Technology. Lecture Notes in Bioengineering. Springer, Singapore. 2021.pp 1-7. https://doi.org/10.1007/978-981-15-6329-4_1
26. Prabhakar, P, Banerjee, M, Verma, S K, Kandar, P. Rapid Extraction and characterization of E. coli phospholipids and study of its potential application in liposomal drug delivery systems. Int J Eng Res Gen Sci.2018; 6(6):34-47.
27. Patle TK, Shrivas K, Kurrey R, Upadhyay S, Jangde R, Chauhan R. Phytochemical screening and determination of phenolics and flavonoids in Dillenia pentagyna using UV–vis and FTIR spectroscopy. Spectrochim Acta Part A. 2020;242:1-10.

https://doi.org/10.1016/j.saa.2020.118717

28. Al-Madhagy SA, Mostafa NM, Youssef FS, Awad GE, Eldahshan OA, Singab AN. Metabolic profiling of a polyphenolic-rich fraction of Coccinia grandis leaves using LC-ESI-MS/MS and in vivo validation of its antimicrobial and wound healing activities. Food & Funct.2019;10(10):6267-75. https://doi.org/10.1039/c9fo01532a
29. Nair SS, Kavrekar V, Mishra A. In vitro studies on alpha amylase and alpha glucosidase inhibitory activities of selected plant extracts. Eur J Exp Bio. 2013;3(1):128-32.
30. Alqahtani AS, Hidayathulla S, Rehman MT, ElGamal AA, Al-Massarani S, Razmovski-Naumovski V, et al. Alpha-amylase and alpha-glucosidase enzyme inhibition and antioxidant potential of 3-oxolupenal and katononic acid isolated from Nuxia oppositifolia. Biomol.2019;10(1):61. https://doi.org/10.3390/biom10010061
31. Sulaiman CT, Gopalakrishnan VK. Radical scavenging and in-vitro hemolytic activity of aqueous extracts of selected acacia species. J App Pharm Sci. 2013;3(3):109-11. https://doi.org/10.7324/JAPS.2013.30321
32. Liu Y, Nair MG. An efficient and economical MTT assay for determining the antioxidant activity of plant natural product extracts and pure compounds. J Nat Pro.2010;73(7):1193-5. https://doi.org/10.1021/np1000945
33. Schneider-Stock, R, & Ribatti, D. The CAM assay as an alternative in vivo model for drug testing. *Organ Mod Drug Dev*.2021;2021:303-323. https://doi.org/10.1007/164_2020_375
34. ImageJ, ver 1.54d, National Institute of Health, Bethesda, Maryland, USA; 2021. Available form https://imagej.net/ij/
35. IBM SPSS Statistics, ver 20.0, International Business Machines, New York, USA; 2021. Available from www.ibm.com/products/spss-statistics
36. Prabhakar, P, Mukherjee, S, Kumar, A, Kumar, S, Verma, DK, Dhara, et al. Optimization of microwave-assisted extraction (MAE) of key phenolic compounds from pigeon pea (Cajanus cajan L.), their characterization, and measurement of their anti-diabetic and cytotoxic potential. J Food Meas Charact.2023a; 17(6):5697-5720. https://doi.org/10.1007/s11694-023-02082-5

37. Begum, SMFM., Fathima, SZ, Priya, S, Sundararajan, R, Hemalatha, S. Screening Indian Medicinal Plants to Control Diabetes – An In silico and In vitro Approach. Gen Med (Los Angeles). 2017; 5:2 https://doi.org/10.4172/2327-5146.1000289

38. Prabhakar, P, Pasayat, AK, Kumar, S, & Banerjee, M. An in silico evaluation of dipeptidyl peptidase-4 (DPP-4) inhibiting potential of Cajanus cajan, Coccinia grandis and Enhydra fluctuans. Proceedings of 2023 International Conference on Communication, Circuits, and Systems (IC3S). 2023 May 26; IEEE; 2023b; pp. 1-6. https://doi.org/10.1109/IC3S57698.2023.10169442

39. Jin X, Luong TL, Reese N, Gaona H, Collazo-Velez V, Vuong C, et al. Comparison of MDCK-MDR1 and Caco-2 cell based permeability assays for anti-malarial drug screening and drug investigations. J Pharmacol Toxicol Methods.2014;70(2):188-94. https://doi.org/10.1016/j.vascn.2014.08.002

40. Prabhakar, P., & Banerjee, M. Nanotechnology in drug delivery system: Challenges and opportunities. J Pharm Sci Res. 2020; 12(4): 492-498.

41. Xiong G, Wu Z, Yi J, Fu L, Yang Z, Hsieh C, et al. ADMETlab 2.0: an integrated online platform for accurate and comprehensive predictions of ADMET properties. Nucleic Acids Res. 2021;49(W1):W5-W14. https://doi.org/10.1093/nar/gkab255

42. Smith MT, Guyton KZ, Gibbons CF, Fritz JM, Portier CJ, Rusyn I, et al. Key characteristics of carcinogens as a basis for organizing data on mechanisms of carcinogenesis. Env Health Pers. 2016;124(6):713-21. https://doi.org/10.1289/ehp.1509912

43. Kar S, Roy K, Leszczynski J. Impact of pharmaceuticals on the environment: risk assessment using QSAR modeling approach. Comp Tox: Method Pro. 2018:395-443. https://doi.org/10.1007/978-1-4939-7899-1_19

44. Tkaczyk A, Bownik A, Dudka J, Kowal K, Ślaska B. Daphnia magna model in the toxicity assessment of pharmaceuticals: A review. Sci Total Env.2021;763:143038. https://doi.org/10.1016/j.scitotenv.2020.143038

45. Mohanty PK, Chourasia N, Bhatt NK, Jaliwala YA. Preliminary phytochemical screening of Cajanus cajan Linn. Asian J Pharm Tech. 2011;1(2):49-52. https://doi.org/10.5958/2231–5713

46. Nowak J, Kiss AK, Wambebe C, Katuura E, Kuźma Ł. Phytochemical analysis of polyphenols in leaf extract from Vernonia amygdalina Delile plant growing in Uganda. App. Sci. 2022;12(2):912. https://doi.org/10.3390/app12020912

47. Prabhakar, P, Mukherjee, S, Kumar, A, Kumar, S, Verma, DK, Dhara, et al. Optimization of MAE for Carica papaya phytochemicals, and its in silico, in vitro, and ex vivo evaluation: for functional food and drug applications. Food Bioscience.2023c; 54:1-21. https://doi.org/10.1016/j.fbio.2023.102861

48. Putra, I M W A, Ate, O T, Kusumawati, I G A W, & Nursini, N W. Antioxidant and inhibition of α-amyalse activities of papasan (Coccinia grandis (L.) Voigt) leaves and Belimbing wuluh (Averrhoa bilimbi L.) fruits combined infusions. J Kim. (J. Chem.).2020; 188-191. https://doi.org/10.24843/JCHEM.2020.v14.i02.p13

49. Packirisamy M, Sivaprakasam M. Coccinia grandis Extract Exerts Antihyperglycemic Effect through its Antioxidant, α-Amylase and α-Glucosidase Inhibitory Activities: An in vitro Study. Asian J Bio Life Sci. 2021;10(3):590-596. https://doi.org/10.5530/ajbls.2021.10.78

50. Bunkrongcheap R, Hutadilok-Towatana N, Noipha K, Wattanapiromsakul C, Inafuku M, Oku H. Ivy gourd (Coccinia grandis L. Voigt) root suppresses adipocyte differentiation in 3T3-L1 cells. Lipids Health and disease. 2014;13(1):1-10. https://doi.org/10.1186/1476-511X-13-88

51. Meenatchi P, Purushothaman A, Maneemegalai S. Antioxidant, antiglycation and insulinotrophic properties of Coccinia grandis (L.) in vitro: Possible role in prevention of diabetic complications. J. Trad. Comp. Med. 2017;7(1):54-64. https://doi.org/10.1016/j.jtcme.2016.01.002

52. Varma, SR, Bhaskar, DA. Antiproliferative activity of Coccinia grandis on cancer cell lines. Eur J Mol Clinical Med.2020;7(10):3895-3900.

53. Zohra, M., & Fawzia, A. Hemolytic activity of different herbal extracts used in Algeria. Int J Pharm. Sci Res.2014; 5(8):495-500.

54. Alencar DB, Melo AA, Silva GC, Lima RL, Pires-Cavalcante K, Carneiro RF, et al. Antioxidant, hemolytic, antimicrobial, and cytotoxic activities of the tropical Atlantic marine zoanthid Palythoa caribaeorum. Anais Acad Bra Ciên. 2015; 87:1113-23. https://doi.org/10.1590/0001-3765201520140370

55. Majumder T, Nagaraju K, Sreelekha K, Nikitha M. Evaluation of Pharmacological Activity of Hydroethanolic Extract Coccinia grandis Linn. Leaves. Sch. Acad. J. Pharm. 2017; 6(4): 149-157. https://doi.org/10.21276/sajp

56. Sankarganesh P, Joseph B, Kumar AG, Illanjiam S, Srinivasan T. Phytomedicinal chemistry and pharmacognostic value of carica papaya L., Leaf. J Pure Appl Microbio. 2018;12(2):751-756. https://doi.org/10.22207/JPAM.12.2.35.

List of Figures

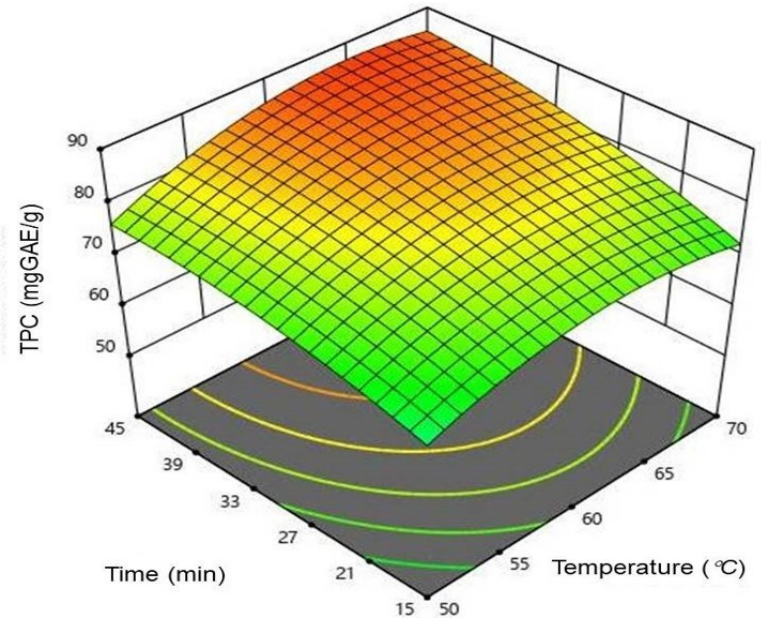

1 (a)

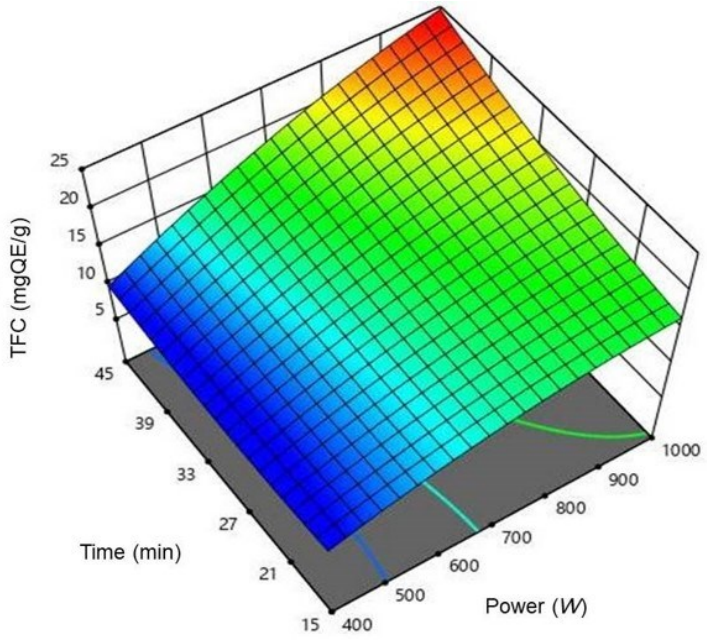

1 (b)

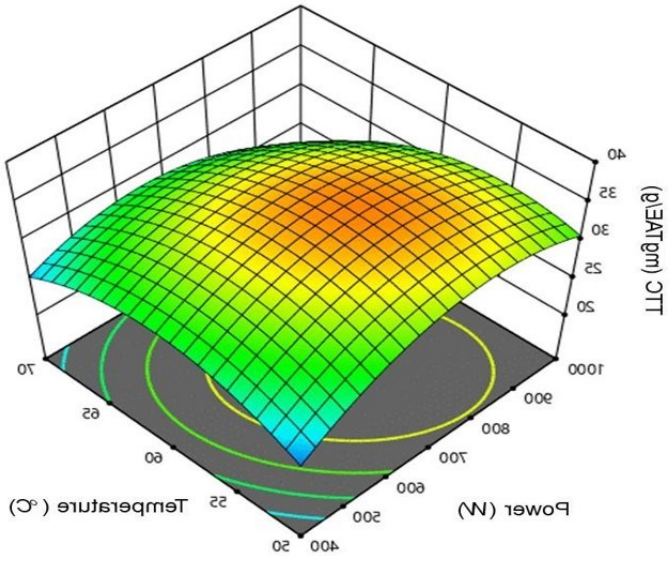

1 (c)

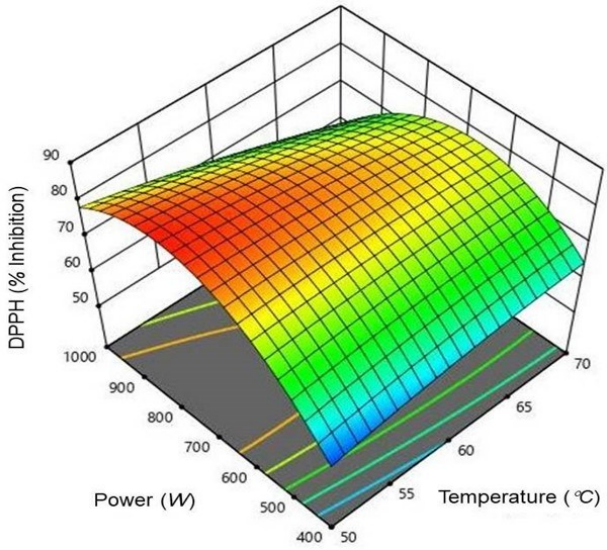

1 (d)

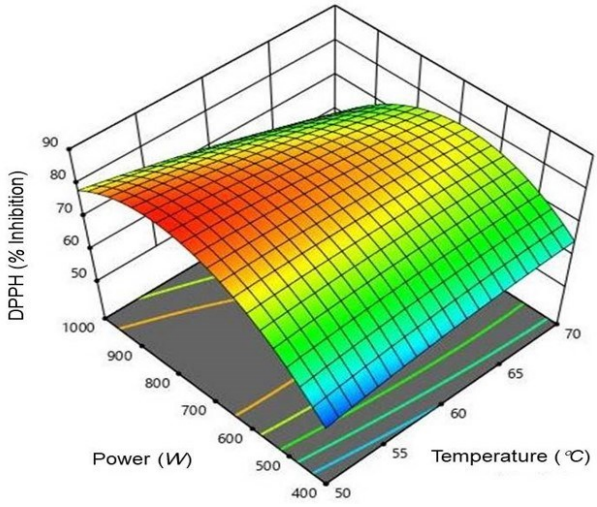

1 (e)

Fig. 1. Illustrations generated using response surface plots on the impact of microwave-assisted extraction parameters on various biochemical parameters include (a) total phenolic content (TPC), (b) total flavonoid content (TFC), (c) total tannin content (TTC), (d) 2,2-diphenyl-1-picrylhydrazyl (DPPH) radical scavenging activity, and (e) Ferric reducing antioxidant power (FRAP)

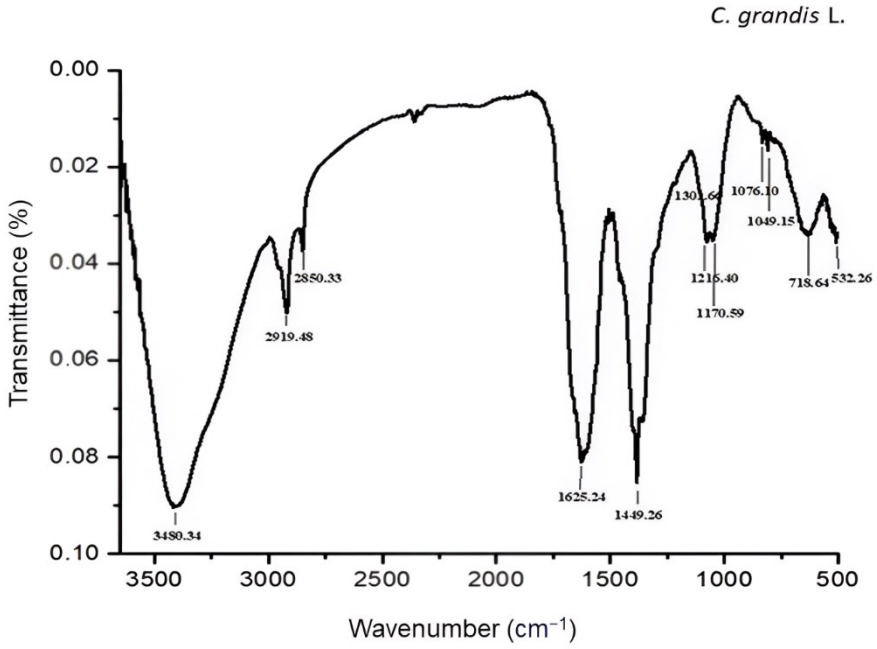

2 (a)

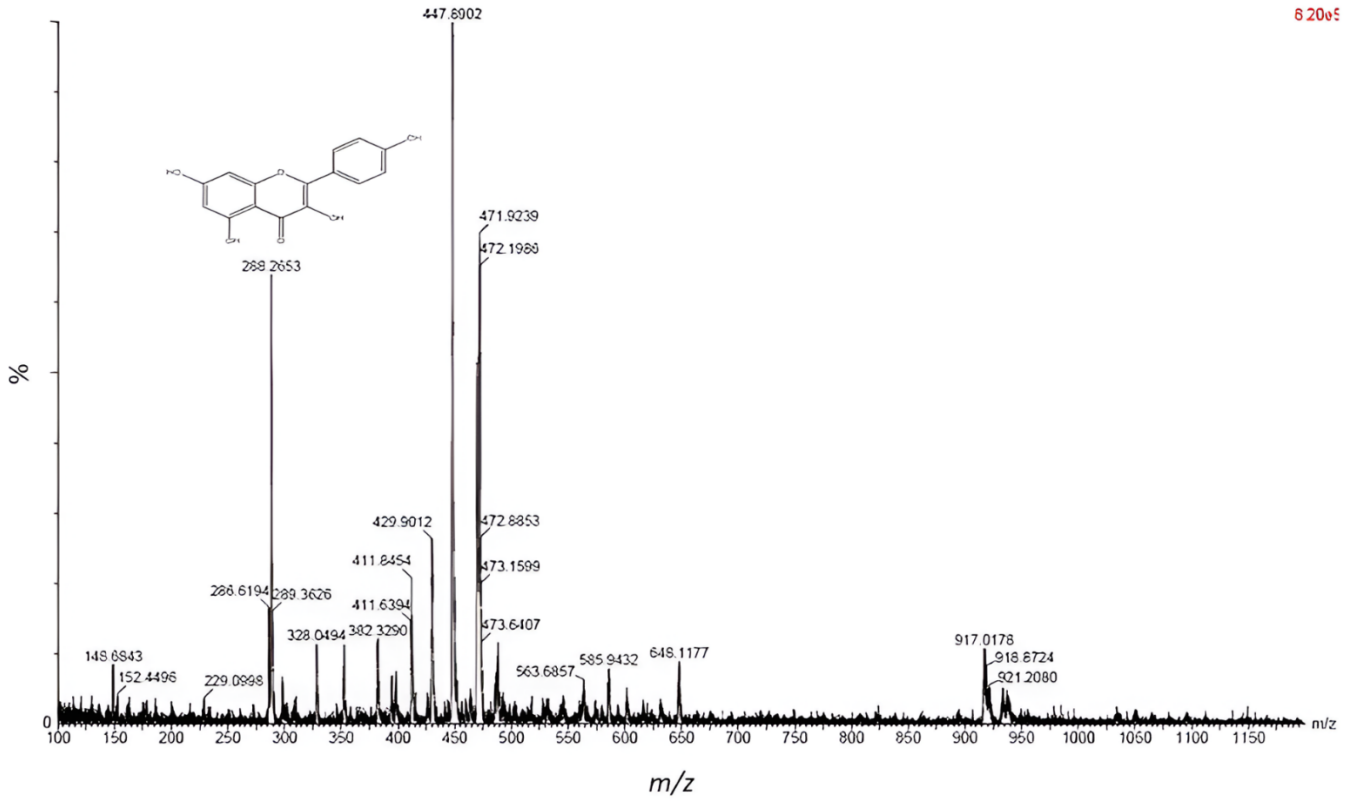

2 (b)

Fig. 2. Two distinct spectra from the spectral analysis that was conducted on the leaf extract of *C. grandis*. The first spectrum, denoted as (a), was obtained using Fourier Transform Infrared (FTIR) spectroscopy. The second spectrum, labeled as (b), was acquired through Liquid Chromatography-Mass Spectrometry (LC-MS) and specifically represents the presence of kaempferol

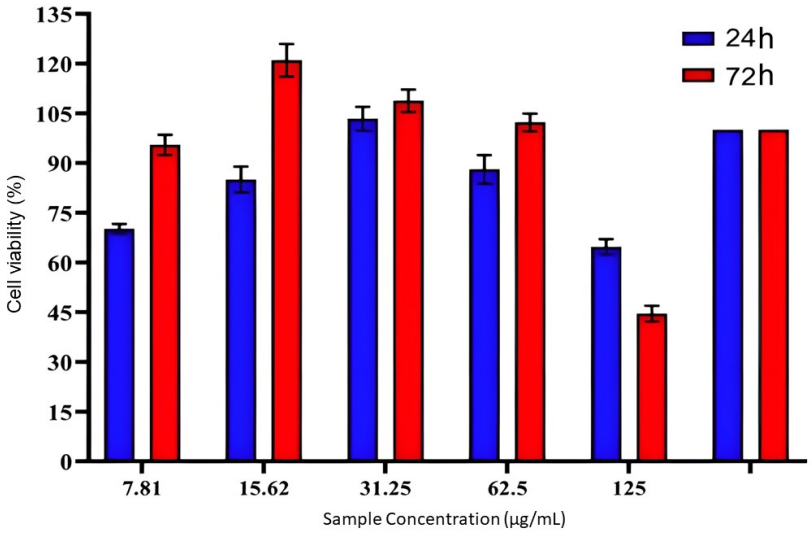

3(a)

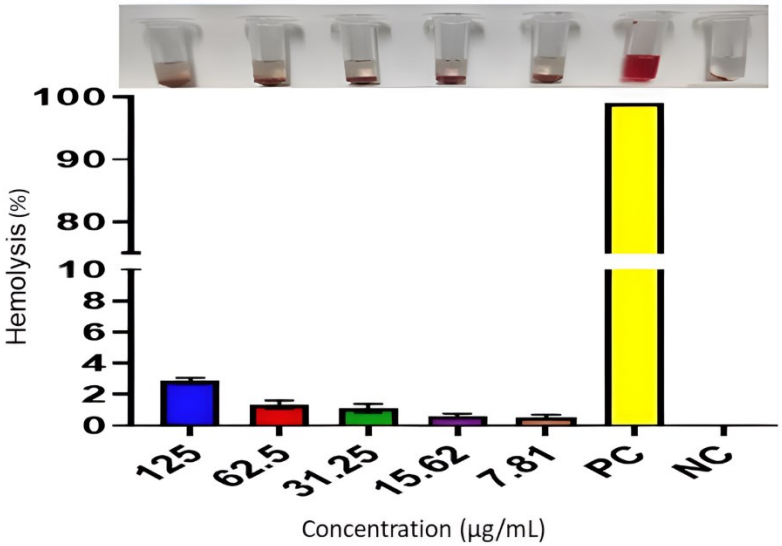

3(b)

Fig. 3. Hemolytic activity and cell viability of varied concentrations of the *C. grandis* leaf extract. (a) Cell viability (%) at different concentrations of the *C. grandis* leaf extract in comparison to the untreated control after 24 and 72 h, and (b) Hemolytic activity (~3.08% hemolysis) of *C. grandis* leaf extract

Fig. 4. Chorioallantoic membrane test (CAM) was performed using the leaf extracts of *C. grandis*. Eggs were given an ethanolic extract of *C. grandis* at several concentrations, ranging from 7.81 to 125 µg/mL, over a period of 0, 48 and 72 h, respectively. There was no evidence of a suppression of vascularization in the sample at any concentration up to 125 µg/mL. The attenuation and degeneration of blood vessels that were not seen at any dose those provide evidence of toxic effects

List of Tables

Table 1. List of the identified phytochemicals from *C. grandis* leaf extract with inhibitory effects against α-amylase and α-glucosidase enzymes and their respective binding affinities

Phytocompounds	Biding affinity in kcal/mol (α-amylase)	Biding affinity in kcal/mol (α-glucosidase)
Benzofuranone	−5.3	−5.1
Campesterol	−7.6	−8.6
Campocatechin	−7.6	−8.5
Coniferyl alcohol	−5.5	−5.1
Ethisterone	−7.2	−7.6
Ferulic acid	−5.8	−5.4
Furanone	−3.8	−3.4
Isosteviol	−7.8	−7.4
Kaempferol	−7.2	−7.1
Luteolin	−7.7	−7.6
Methyl caffeate	−7.7	−7.6
p-coumaric acid	−5.5	−5.5
Quercetin	−7.8	−7.0
Listroside	−7.7	−7.6
Lukianol	−7.7	−8.0
Oleuropein	−7.7	−7.6
Sinapic acid	−5.6	−5.6
Stigmasterol	−7.7	−8.4
Undecanol	−4.1	−3.7

Table 2. Analyzed and interpreted results from the study employing the Box-Behnken design for the experimental setup and analysis of the response variables associated with the microwave-assisted extraction of *C. grandis* leaves

RUN	Temperature (°C)	Power (W)	Time (min)	TPC (mgGAE/g DM)	TFC (mgQE/g DM)	TTC (mgTAE/g DM)	DPPH (% Inhibition)	FRAP (mgTE/g DM)
1	60	700	30	88.933	14.133	33.36	83.964	100.098
2	60	700	30	81.28	13.84	33.973	78.59	95.146
3	60	700	30	81.733	13.91	36.506	83.853	101.991

4	60	400	45	76.981	10.091	29.693	63.749	80.133
5	50	700	45	73.733	22.933	32.826	86.388	106.866
6	70	400	30	68.24	9.88	25.306	66.631	79.946
7	60	700	30	80.733	18.8	37.573	82.096	100.546
8	70	1000	30	63.87	22.986	22.653	58.902	69.373
9	70	700	45	85.786	19.04	29.373	80.451	100.373
10	50	400	30	60.72	10.84	23.626	57.222	74.32
11	60	1000	45	68.946	24.16	30.24	72.853	73.946
12	60	1000	15	54.453	16.266	27.306	64.069	64.586
13	70	700	15	74.933	16.826	23.146	68.784	89.37
14	60	400	15	65.6	9.786	26.093	55.659	59.08
15	60	700	30	80.866	17.466	35.546	82.43	99.56
16	50	1000	30	62.933	21.546	30.893	76.562	81.64
17	50	700	15	67.906	15.986	28.96	79.631	89.64

Note: All the experiments were done in triplicate and the average value of the response variables are expressed in the table.

Table 3. The analysis of variance (ANOVA) to assess the statistical significance of the response variables and the regression coefficients of the second-order model fitted for the leaf extract of *C. grandis*

Terms	TPC (mgGAE/g DM)	TFC (mgQE/g DM)	TTC (mgTAE/g DM)	DPPH (% Inhibition)	FRAP (mgTE/g DM)
Intercept					
β_0	82.71	15.63	35.39	82.19	99.47
Linear					
β_1	3.44*	-0.3216	-1.98**	-3.13**	-1.68*
β_2	-2.67	5.55**	0.7968	3.64**	-0.4917
β_3	5.32**	2.17*	2.08**	4.41**	7.33**
Quadratic					

β_{11}	-4.84*	2.15	-4.76**	-1.31	1.99
β_{22}	-13.93**	-1.47	-5.01**	-16.04**	-25.14**
β_{33}	-2.28	0.9146	-2.05*	-2.06	-4.89**
Interaction					
β_{12}	-1.65	0.6000	-2.48*	-6.77**	-4.47325**
β_{13}	1.26	-1.18	0.5902	1.23	-1.55575
β_{23}	0.7780	1.90	-0.1665	0.1735	-2.92325*
CV (%)	5.44	11.50	5.02	2.96	2.23
p-value (Regression)	0.003**	0.002**	0.0006**	<0.0001**	<0.0001**
p-value (Lack of fit)	0.31	0.18	0.38	0.96	0.97

Table 4. The regression equation to predict the values of the response variables based on the values of the predictor variables using the mathematical model representing the relationship between the predictor variables and the response variables

Response	Model	R^2
TPC	$82.71+3.44x_1-2.67x_2+5.32x_3-4.84x_1^2-13.93x_2^2-2.28x_3^2-1.65x_{12}+1.26x_{13}-0.77x_{23}$	0.92
TFC	$15.63-0.32x_1+5.55x_2+2.17x_3-2.15x_1^2-1.47x_2^2+0.91x_3^2+0.60x_{12}-1.18x_{13}+1.90x_{23}$	0.93
TTC	$35.39-1.98x_1+0.79x_2+2.08x_3-4.76x_1^2-5.01x_2^2-2.05x_3^2-2.48x_{12}+0.59x_{13}+0.16x_{23}$	0.95
DPPH	$82.19-3.13x_1+3.64x_2+4.41x_3-1.31x_1^2-16.04x_2^2-2.06x_3^2-6.77x_{12}+1.23x_{13}+0.17x_{23}$	0.98
FRAP	$99.47+1.68x_1-0.49x_2+7.3x_3+1.99x_1^2-25.14x_2^2-4.89x_3^2-4.47x_{12}-1.55x_{13}-2.92x_{23}$	0.99

Supplementary Figures and Tables

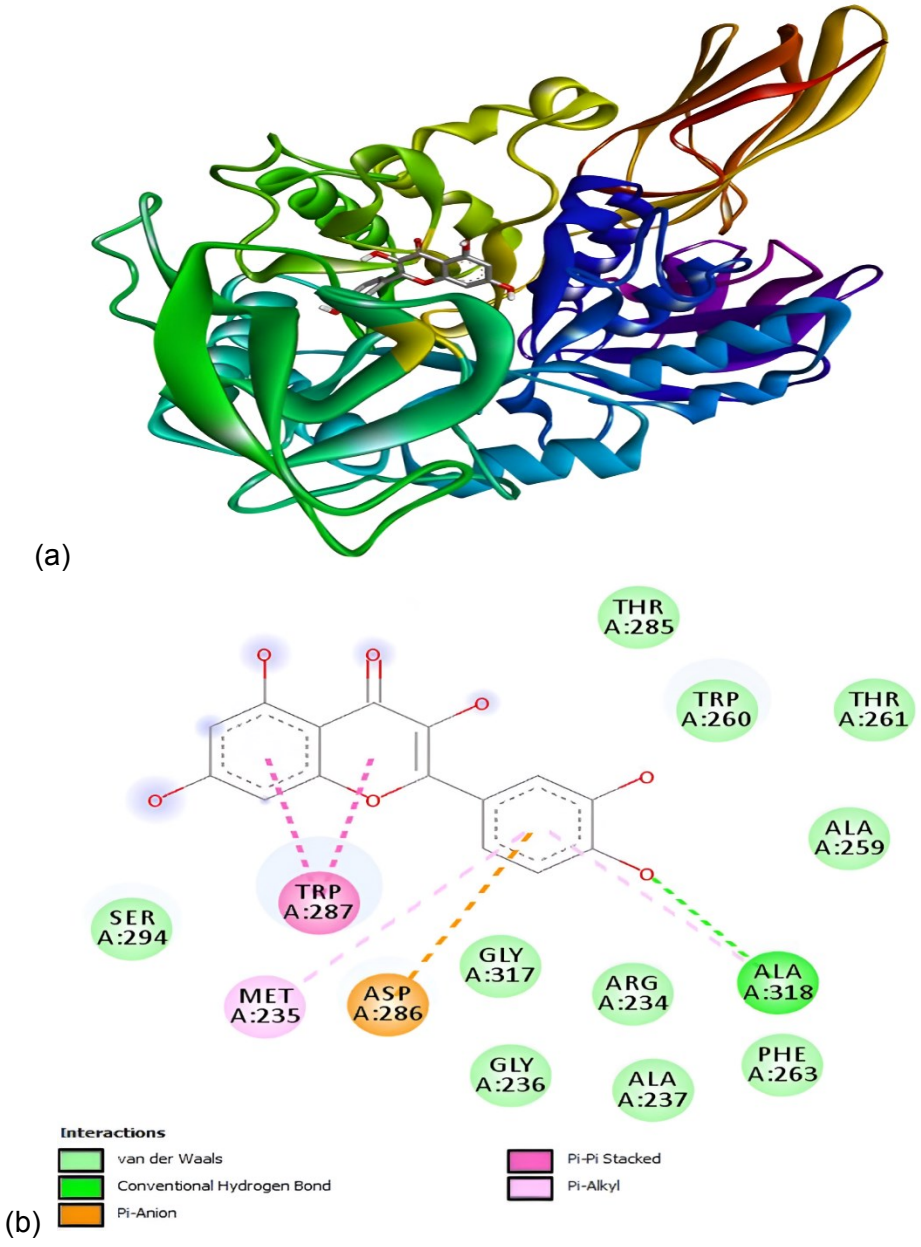

Fig. S1. The molecular interactions between an enzyme-phytochemical complex can be described as follows: (a) The three-dimensional ribbon structure of α-amylase interacting with quercetin reveals the binding pose at the active site of the α-amylase enzyme, including the specific amino

acid residues involved in the interaction. (b) The two-dimensional structure illustrates the various types of bonds formed between the enzyme and quercetin, along with their respective bond orders, which range from 2.54 to 5.0 Å

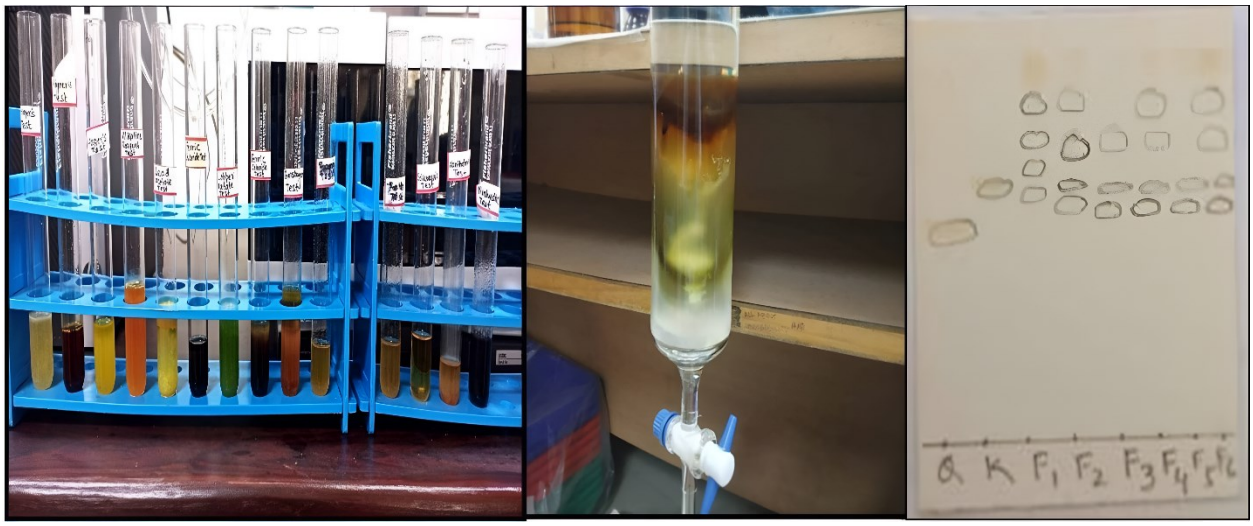

(a) (b) (c)

Fig. S2. Illustrations on the process involved in the analysis of phytochemicals from *C. grandis* leaf extract include three main steps: (a) preliminary phytochemical screening; (b) column chromatography; and (c) identification of the presence of kaempferol using thin layer chromatography

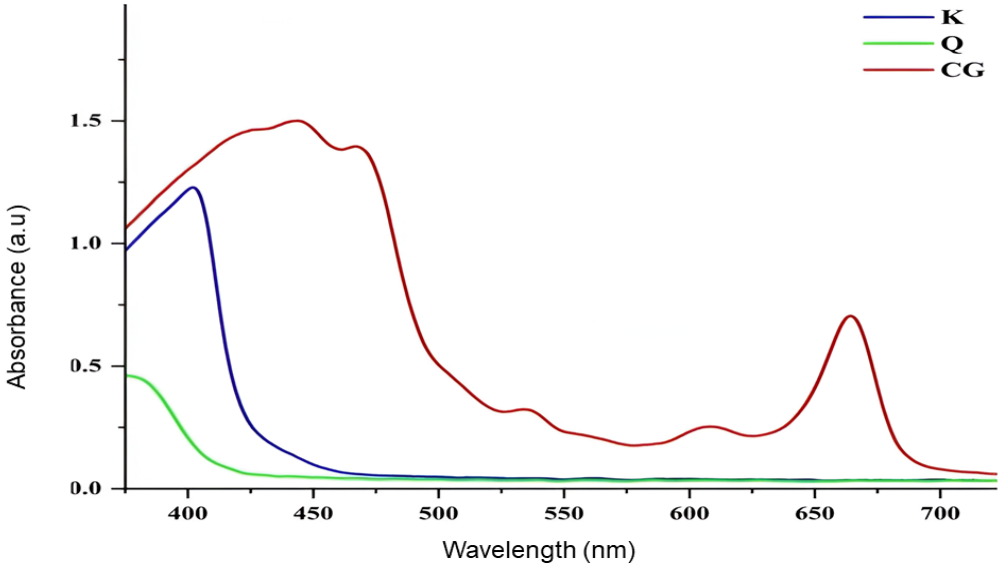

Fig. S3. Spectra on the existence of phenolic compounds and flavonoids from *C. grandis* leaf extract using UV-visible spectra analysis. [***Abbreviations:*** K: Kaempferol, Q: Quercetin, CG: *C. grandis*]

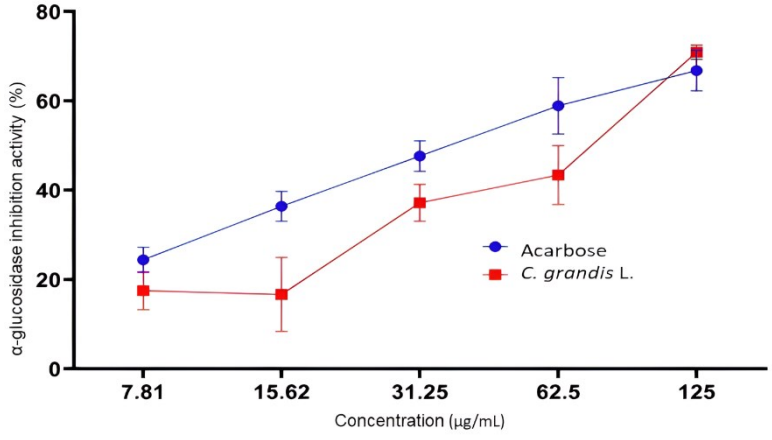

(a)

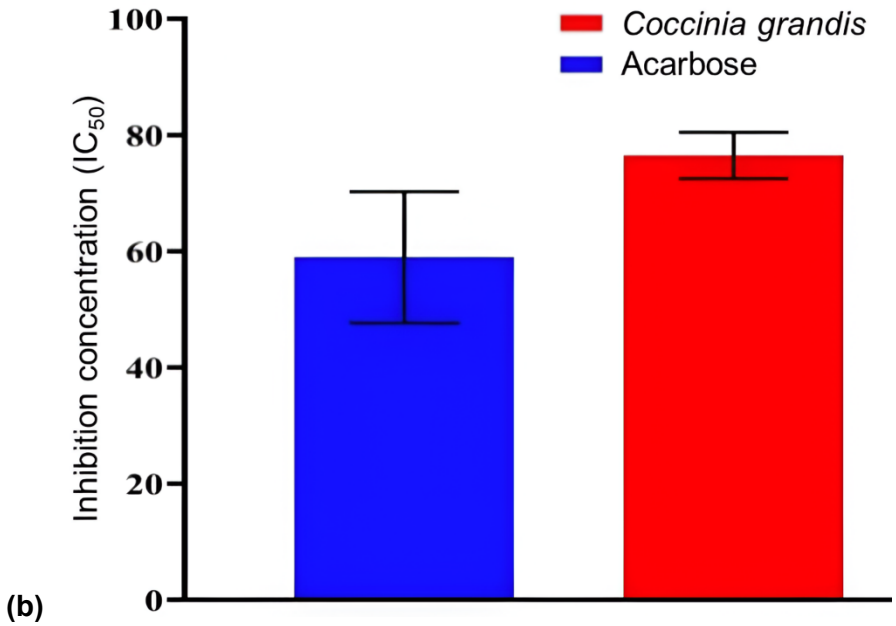

Fig. S4. Graphical representation of α-glucosidase inhibitory activity (a) percentage inhibition (70.89±1.6 %) of α-glucosidase at each concentration of *C. grandis* leaf extract in comparison with acarbose and (b) its half-minimal concentration IC_{50} (46.49±3.97 μg/mL). [*Note:* All the values are expressed in means of the triplicate (*N*=3, $p<0.05$)

Table S1. Insights into the molecular architecture and crystallographic data collected by the protein data bank (PDB) from enzymes, along with their corresponding PDB identifiers (PBD ID), central grid values, and resolution

Enzyme	PDB ID	Centre Grid (X, Y, Z) in Å	Resolution (X-ray Diffraction) in Å	Exhaustiveness
α-amylase	3bc9	47.788286, 25.075619, 5.722952	1.35	100
α-glucosidase	1obb	30.179130, 33.953391, 22.922000	1.90	100

Table S2. The analysis of the absorption and distribution characteristics of phytochemicals from leaf extract of C. grandis on evaluating their anticipated permeability and bioavailability across various physiological barriers

Phytochemicals	HIA	Caco-2 Permeability	BBBP	p-glycoprotein inhibitor	p-glycoprotein substrate	MDCK Permeability	F20 %	F30 %	PPB %	VD	Fu %
Benzofuranone	0.006	−4.594	0.239	0.001	0.255	2.2e-05	0.888	0.906	92.28	0.849	10.170
Campesterol	0.004	−4.740	0.854	0.377	0.001	9e-06	0.013	0.243	98.61	1.842	1.789
Campocatechin	0.004	−4.930	0.529	0.013	0.005	2.7e-05	0.002	0.003	90.80	0.525	3.310
Coniferyl alcohol	0.010	−4.457	0.295	0.001	0.321	1.8e-05	0.005	0.742	80.73	1.059	16.950
Ethisterone	0.008	−4.725	0.964	0.104	0.000	2.1e-05	0.553	0.004	95.28	1.034	1.424
Ferulic acid	0.030	−4.902	0.329	0.000	0.086	1.5e-05	0.047	0.584	89.75	0.339	6.394
Furanone	0.006	−4.446	0.219	0.000	0.022	2.2e-05	0.015	0.008	79.21	2.455	38.780
Isosteviol	0.006	−5.285	0.221	0.009	0.000	1.7e-05	0.002	0.890	91.25	0.558	9.029
Kaempferol	0.008	−4.974	0.009	0.004	0.001	9e-06	0.856	0.993	97.86	0.522	4.411
Luteolin	0.047	−5.028	0.009	0.004	0.274	1e-05	0.998	1.000	95.43	0.533	5.984
Methyl caffeate	0.020	−4.631	0.185	0.001	0.077	2e-05	0.025	0.806	85.83	0.390	10.410
p-coumaric acid	0.009	−4.961	0.290	0.000	0.017	1.3e-05	0.004	0.194	85.36	0.293	13.720
Quercetin	0.014	−5.204	0.008	0.004	0.005	8e-06	0.930	0.997	95.49	0.579	7.423
Listroside	0.927	−5.702	0.596	0.000	0.673	0.000102	0.100	0.998	63.72	0.394	34.460
Lukianol	0.007	−4.744	0.010	0.048	0.006	1.3e-05	0.943	0.537	101.10	0.414	0.795
Oleuropein	0.950	−5.847	0.672	0.000	0.842	0.000103	0.371	0.998	74.00	0.568	25.640
Sinapic acid	0.165	−4.962	0.271	0.001	0.040	1.3e-05	0.189	0.624	88.79	0.450	9.389
Stigmasterol	0.005	−4.668	0.691	0.066	0.001	8e-06	0.008	0.185	98.67	2.408	1.572
Undecanol	0.003	−4.414	0.890	0.004	0.012	2.2e-05	0.261	0.979	93.51	1.628	5.165

Abbreviations: HIA: Human Intestinal Absorption [Category 1: HIA+(HIA < 30 %); Category 0: HIA-(HIA < 30 %); The output value is the probability of being HIA+within the range of 0 to 1, Caco-2 Permeability: Optimal: higher than -5.15 log cm/s]; BBBP: Blood-Brain Barrier Penetration [Category

1: BBB+; Category 0: BBB-; The output value is the probability of being BBB+,within the range of 0 to 1, p-glycoprotein inhibitor: Category 1: Inhibitor; Category 0: Non-inhibitor; The output value is the probability of being p-glycoprotein inhibitor, within the range of 0 to 1, p-glycoprotein substrate: Category 1: substrate; Category 0: Non-substrate; The output value is the probability of being p-glycoprotein substrate, within the range of 0 to 1]; MDCK Permeability: Madin−Darby Canine Kidney cells [Low permeability: < 2 × 10^{-6} cm/s, medium permeability: 2-20 × 10^{-6} cm/s, high passive permeability: > 20 × 10^{-6} cm/s, F20 %: 20 % Bioavailability Category 1: F20 %+ (bioavailability < 20 %); Category 0: F20 %- (bioavailability≥20 %); The output value is the probability of being F20 %+,within the range of 0 to 1, F30 %: 30 % Bioavailability; Category 1: F30 %+ (bioavailability < 30 %); Category 0: F30 %- (bioavailability ≥30 %); The output value is the probability of being F30 %+,within the range of 0 to 1]; PPB: Plasma Protein Binding [Optimal: < 90 %. Drugs with high protein-bound may have a low therapeutic index]; VD: Volume Distribution [Optimal: 0.04-20L/kg]; Fu: Fraction unbound [In plasma; Low: <5 %; Middle: 5~20 %; High: > 20 %].

Table S3. The metabolic profile of phytochemicals in *C. grandis* with various substrates and inhibitors of the cytochrome P450 enzyme family and the obtained values on the characterization of their metabolism insight into the specific metabolic pathways and interactions involved in the biotransformation of these phytochemicals

Phytochemicals	CYP1A2 inhibitor	CYP1A2 substrate	CYP2C19 inhibitor	CYP2C19 substrate	CYP2C9 inhibitor	CYP2C9 substrate	CYP2D6 inhibitor	CYP2D6 substrate	CYP3A4 inhibitor	CYP3A4 substrate
Benzofuranone	0.914	1.716	0.156	0.091	0.044	0.776	0.161	0.774	0.018	0.215
Campesterol	0.055	0.523	0.071	0.957	0.093	0.216	0.005	0.445	0.181	0.769
Campocatechin	0.928	0.767	0.629	0.346	0.554	0.429	0.054	0.458	0.298	0.419
Coniferyl alcohol	0.709	0.867	0.042	0.422	0.032	0.836	0.019	0.893	0.087	0.241
Ethisterone	0.107	0.846	0.891	0.93	0.445	0.23	0.093	0.142	0.639	0.93
Ferulic acid	0.059	0.478	0.042	0.057	0.142	0.367	0.02	0.199	0.026	0.075
Furanone	0.205	0.147	0.048	0.072	0.014	0.399	0.018	0.597	0.008	0.179
Isosteviol	0.005	0.855	0.016	0.901	0.089	0.254	0.007	0.157	0.26	0.078
Kaempferol	0.972	0.11	0.181	0.046	0.653	0.867	0.722	0.283	0.697	0.08
Luteolin	0.981	0.154	0.124	0.046	0.576	0.842	0.568	0.559	0.549	0.092
Methyl caffeate	0.899	0.696	0.252	0.078	0.436	0.86	0.164	0.732	0.292	0.227

p-coumaric acid	0.061	0.067	0.046	0.052	0.232	0.566	0.019	0.169	0.031	0.08
Quercetin	0.943	0.115	0.053	0.041	0.598	0.643	0.411	0.205	0.348	0.046
Listroside	0.014	0.077	0.045	0.204	0.016	0.145	0.012	0.084	0.21	0.2
Lukianol	0.885	0.104	0.769	0.043	0.491	0.889	0.289	0.871	0.308	0.23
Oleuropein	0.017	0.071	0.035	0.071	0.014	0.582	0.003	0.12	0.357	0.157
Sinapic acid	0.046	0.833	0.026	0.063	0.053	0.277	0.016	0.198	0.01	0.084
stigmasterol	0.041	0.603	0.074	0.954	0.106	0.132	0.038	0.643	0.339	0.852
Undecanol	0.905	0.319	0.401	0.07	0.281	0.865	0.01	0.077	0.058	0.074

Note: Category 0: Non-substrate / Non-inhibitor; Category 1: substrate / inhibitor. The output value is the probability of being substrate / inhibitor, within the range of 0 to 1.

Table S4. Results on toxicological impacts of phytochemicals derived from *C. grandis* in the human body using physiological toxicity profiles of different toxicity assays

Phytochemicals	hERG Blockers	Hepatotoxicity	DILI	Ames Toxicity	Rat Oral Acute Toxicity	FDAMDD	Skin Sensitization	Carcinogenicity	Eye corrosion	Eye Irritation	Respiratory Toxicity
Benzofuranone	0.013	0.582	0.582	0.266	0.422	0.032	0.391	0.835	0.742	0.991	0.638
Campesterol	0.04	0.193	0281	0.032	0.023	0.645	0.176	0.067	0.003	0.01	0.502
Campocatechin	0.162	0.753	0.414	0.744	0.876	0.908	0.04	0.562	0.003	0.014	0.036
Coniferyl alcohol	0.035	0.17	0.045	0.141	0.386	0.09	0.949	0.662	0.493	0.987	0.502
Ethisterone	0.041	0.149	0.18	0.015	0.163	0.884	0.032	0.916	0.004	0.023	0.961
Ferulic acid	0.023	0.345	0.511	0.114	0.733	0.076	0.929	0.443	0.515	0.979	0.72
Furanone	0.02	0.13	0.126	0.071	0.877	0.016	0.293	0.908	0.985	0.996	0.906

Isosteviol	0.002	0.422	0.027	0.033	0.082	0.132	0.012	0.102	0.004	0.507	0.949
Kaempferol	0.07	0.098	0.979	0.672	0.156	0.109	0.856	0.097	0.009	0.929	0.09
Luteolin	0.064	0.084	0.905	0.536	0.046	0.741	0.946	0.095	0.009	0.944	0.22
Methyl caffeate	0.034	0.244	0.082	0.375	0.801	0.234	0.94	0.392	0.046	0.461	0.448
p-coumaric acid	0.025	0.673	0.2	0.045	0.796	0.031	0.941	0.151	0.672	0.988	0.512
Quercetin	0.099	0.1	0.98	0.657	0.065	0.31	0.919	0.05	0.007	0.936	0.072
Listroside	0.005	0.168	0.954	0.693	0.088	0.147	0.032	0.954	0.003	0.007	0.643
Lukianol	0.106	0.25	0.976	0.012	0.1	0.385	0.206	0.099	0.003	0.106	0.064
Oleuropein	0.003	0.127	0.954	0.781	0.136	0.2	0.028	0.953	0.003	0.007	0.72
Sinapic acid	0.018	0.363	0.21	0.016	0.321	0.055	0.949	0.278	0.391	0.94	0.428
Stigmasterol	0.012	0.011	0.055	0.029	0.054	0.539	0.025	0.054	0.003	0.001	0.19
Undecanol	0.106	0.016	0.04	0.007	0.041	0.013	0.926	0.066	0.991	0.971	0.341

Abbreviations: hERG: human ether-a-go-go related gene [Blockers: Category 1: active; Category 0: inactive; The output value is the probability of being active, within the range of 0 to 1, Hepatotoxicity: Category 1: Hepatotoxicity positive(+); Category 0: Hepatotoxicity negative(-); The output value is the probability of being toxic, within the range of 0 to 1]; DILI: Drug-induced liver injury [Category 1: drugs with a high risk of DILI; Category 0: drugs with no risk of DILI. The output value is the probability of being toxic, within the range of 0 to 1, Ames Toxicity: Category 1: Ames positive(+); Category 0: Ames negative(-); The output value is the probability of being toxic, within the range of 0 to 1, Rat Oral Acute Toxicity: Category 0: low-toxicity; Category 1: high-toxicity; The output value is the probability of being highly toxic, within the range of 0 to 1]; FDAMDD: Food and Drug Administration recommended Maximum Daily Drug Dose [Category 1: FDAMDD (+); Category 0: FDAMDD (-);The output value is the probability of being positive, within the range of 0 to 1, Skin Sensitization: Category 1: Sensitizer; Category 0: Non-sensitizer; The output value is the probability of being sensitizer, The output value is the probability of being sensitizer, within the range of 0 to 1, Carcinogenicity: Category 1: carcinogens; Category 0: non-carcinogens; The output value is the probability of being toxic, within the range of 0 to 1, Eye corrosion: Category 1: corrosives ; Category 0: noncorrosive; The output value is the probability of being corrosives, within the range of 0 to 1, Eye Irritation: Category 1: irritants ; Category 0: nonirritants; The output value is the probability of being irritants, within the range of 0 to 1, Respiratory Toxicity: Category 1: respiratory toxicants; Category 0:respiratory nontoxicants; The output value is the probability of being toxic, within the range of 0 to 1].

Table S5. Results on the specific mechanism to predict the toxicity of compounds derived from *C. grandis* employing the Tox21 pathway for assessing the impact of these compounds on both nuclear pathways and stress response pathways

Phytochemicals	NR-AR	NR-AR-LBD	NR-AhR	NR-Aromatase	NR-ER	NR-ER-LBD	NR-PPAR gamma	SR-ARE	SR-ATAD5	SR-HSE	SR-MMP	SR-p53
Benzofuranone	0.013	0.005	0.375	0.01	0.29	0.008	0.004	0.528	0.016	0.06	0.346	0.067
Campesterol	0.002	0.003	0.0	0.012	0.397	0.933	0.008	0.123	0.001	0.046	0.89	0.014
Campocatechin	0.027	0.626	0.625	0.905	0.489	0.256	0.808	0.86	0.6	0.715	0.851	0.97
Coniferyl alcohol	0.033	0.014	0.613	0.08	0.152	0.011	0.011	0.482	0.176	0.239	0.317	0.422
Ethisterone	0.765	0.919	0.005	0.589	0.671	0.865	0.563	0.699	0.045	0.588	0.965	0.855
Ferulic acid	0.809	0.278	0.277	0.021	0.254	0.033	0.07	0.525	0.19	0.296	0.22	0.171
Furanone	0.029	0.003	0.017	0.004	0.168	0.006	0.002	0.073	0.006	0.019	0.023	0.005
Isosteviol	0.265	0.044	0.003	0.578	0.132	0.061	0.858	0.135	0.045	0.239	0.571	0.091
Kaempferol	0.008	0.371	0.967	0.941	0.959	0.985	0.963	0.873	0.612	0.557	0.968	0.921
Luteolin	0.079	0.169	0.977	0.908	0.954	0.996	0.939	0.884	0.675	0.888	0.976	0.891
Methyl caffeate	0.735	0.655	0.912	0.195	0.572	0.855	0.375	0.905	0.8	0.892	0.827	0.796
p-coumaric acid	0.857	0.349	0.229	0.011	0.477	0.432	0.012	0.783	0.153	0.237	0.318	0.347
Quercetin	0.01	0.179	0.967	0.917	0.927	0.987	0.961	0.815	0.436	0.655	0.962	0.888
Listroside	0.006	0.241	0.035	0.032	0.186	0.013	0.048	0.161	0.202	0.017	0.0715	0.44
Lukianol	0.078	0.567	0.915	0.965	0.981	0.996	0.975	0.948	0.706	0.482	0.989	0.93
Oleuropein	0.006	0.185	0.111	0.044	0.187	0.011	0.251	0.329	0.298	0.06	0.728	0.42
Sinapic acid	0.226	0.153	0.205	0.393	0.198	0.013	0.829	0.57	0.483	0.357	0.28	0.678
stigmasterol	0.0	0.002	0.0	0.005	0.369	0.923	0.005	0.135	0.001	0.052	0.943	0.015
Undecanol	0.016	0.002	0.006	0.041	0.0288	0.017	0.04	0.066	0.004	0.519	0.051	0.031

Abbreviations: NR-AR (Nuclear-hormone Receptor; androgen receptor): Category 1: actives ; Category 0: inactives; The output value is the probability of being active, within 0 and 1, NR-AR-LBD (Nuclear-hormone Receptor; Androgen receptor-Ligand binding domain): Category 1: actives ; Category 0: inactives; The output value is the probability of being active, within 0 and 1,NR-AhR (Nuclear-hormone Receptor-Aryl

hydrocarbon receptor): Category 1: actives ; Category 0: inactives; The output value is the probability of being active, NR-Aromatase: Category 1: actives ; Category 0: inactives; The output value is the probability of being active, within 0 and 1, NR-ER (Nuclear hormone receptor-Estrogen receptor): Category 1: actives ; Category 0: inactives; The output value is the probability of being active, within 0 and 1 NR-ER-LBD (Nuclear hormone Receptor-Estrogen receptor ligand-binding domain) Category 1: actives ; Category 0: inactives; The output value is the probability of being active, within 0 and 1 NR-PPAR-gamma(Nuclear hormone-Peroxisome proliferator-activated receptor gamma): Category 1: actives ; Category 0: inactives; The output value is the probability of being active, within 0 and 1 SR-ARE (Antioxidant response element): Category 1: actives ; Category 0: inactives; The output value is the probability of being active, within 0 and 1 SR-ATAD5 (ATPase family AAA domain-containing protein 5) Category 1: actives ; Category 0: inactives; The output value is the probability of being active, within 0 and 1, SR-HSE(Heat shock factor response element Category 1: actives ; Category 0: inactives; The output value is the probability of being active, within 0 and 1 SR-MMP(Mitochondrial membrane potential Category 1: actives ; Category 0: inactives; The output value is the probability of being active, within 0 and 1, SR-p53(Category 1: actives ; Category 0: inactives; The output value is the probability of being active, within 0 and 1, Empirical decision: 0-0.3: excellent; 0.3-0.7: medium; 0.7-1.0: poor]

Table S6. Results on the process of eliminating and studying the harmful effects of phytochemicals derived from *C. grandis* on the external environment in understanding their excretion dynamics and environmental toxicology

Phytochemicals	Clearance	Half Life (t1/2)	Bioconcentration Factors	IGC_{50}	$LC_{50}FM$	$LC_{50}DM$
Benzofuranone	11.101	0.83	0.718	2.999	3.449	4.352
Campesterol	17.948	0.0015	3.141	4.855	4.972	5.897
Campocatechin	6.862	0.332	1.379	4.15	6.075	5.553
Coniferyl alcohol	12.341	0.92	0.707	2.958	3.625	3.913
Ethisterone	5.594	0.208	0.559	2.81	2.71	4.556
Ferulic acid	7.48	0.926	0.454	3.086	3.249	3.908
Furanone	14.22	0.894	0.522	2.235	2.799	3.76
Isosteviol	0.344	0.503	0.212	3.28	3.215	4.207
Kaempferol	6.868	0.905	0.986	4.386	5.223	5.205
Luteolin	8.146	0.898	1.016	4.432	5.222	5.302
Methyl caffeate	15.624	0.93	0.657	3.886	0.047	4.92

p-coumaric acid	6.299	0.919	0.416	3.136	3.373	3.775
Quercetin	8.284	0.929	1.017	4.231	5.222	5.331
Listroside	2.057	0.647	0.519	3.099	4.572	5.312
Lukianol	6.776	0.276	1.856	5.61	6.248	6.491
Oleuropein	2.585	0.832	0.556	3.52	4.591	5.383
Sinapic acid	7.776	0.933	0.472	2.765	3.002	3.951
stigmasterol	15.958	0.014	3.367	4.978	5.511	6.355
Undecanol	7.769	0.409	1.871	4.853	4.811	3.82

Note: Clearance: High: >15 mL/min/kg; moderate: 5-15 mL/min/kg; low: < 5 mL/min/kg, Half-Life (t1/2): Category 1: long half-life; Category 0: short half-life; long half-life: > 3h; short half-life: <3h; The output value is the probability of having long half-life, within 0 and 1, Bioconcentration factors: Bioconcentration factors are used for considering secondary poisoning potential and assessing risks to human health via the food chain. The unit of BCF is log10 (L/kg), IGC_{50}: Tetrahymena pyriformis 50 percent growth inhibition concentration. LC_{50}FM 96-*h* fathead minnow 50 percent lethal concentration, LC_{50}DM: 48-*h* daphnia magna 50 percent lethal concentration

Table S7. Predicted and validated values obtained from the optimized conditions of MAE of Coccinia leaf samples in terms of total phenolic content (TPC), total flavonoid content (TFC), total tannin content (TTC), 2,2-diphenyl-1-picrylhydrazyl (DPPH) radical scavenging activity, and (E) ferric reducing antioxidant power (FRAP)

Responses	Experimental Value	RSM Predicted Optimized Value	Relative Error (%)
TPC (mgGAE/g DM)	79.86	81.87	2.4
TFC (mgQE/g DM)	23.12	21.24	8.85
TTC (mgTAE/g DM)	35.03	35.24	0.59
DPPH (% Inhibition)	83.62	85.83	2.5
FRAP (mgTE/g DM)	101.56	102.27	0.69

Table S8. Results obtained from the leaf extract from *C. grandis* using liquid-chromatography-mass spectrometry analysis that involved the identification of phytochemicals achieved by analyzing the distinct mass-to-charge ratio values of the phytochemicals, along with their corresponding retention times

S.N.	Phytocompounds	Molecular Formula	Compound Types	Retention Time (*min*)	Parent Ion (*m/z*)	Ionization Mode
1	Benzofuranone	$C_8H_6O_2$	Furan	5.6	136.36	Negative
2.	Camptothecin	$C_{20}H_{16}N_2O_4$	Quinoline	28.04	348.70	Negative
4.	Coniferyl alcohol	$C_{10}H_{12}O_3$	Alcohol	30.34	180.54	Negative
5.	Ethisterone	$C_{10}H_{12}O_3$	Steroid	11.60	310.14	Negative
6.	Ferulic acid	$C_{10}H_{10}O_4$	Cinnamic acid	12.63	194.63	Negative
8.	Isosteviol	$C_{20}H_{30}O_3$	Terpenoid	39.58	316	Negative
9.	Kaempferol	$C_{15}H_{10}O_6$	Flavonoid	15.10	286.16	Positive
10.	Luteolin	$C_{15}H_{10}O_6$	Flavone	17.22	286.20	Positive
11.	Methyl caffeate	$C_{10}H_{10}O_4$	Caffeate ester	14.67	194.70	Negative
12.	*p*-coumaric acid	$C_9H_8O_3$	Coumarin	3.95	164.15	Positive
14	Sinapic acid	$C_{11}H_{12}O_5$	Cinnamic acid	20.34	224.71	Negative

15	Stigmasterol	$C_{29}H_{48}O$	Sterol	27.01	412.05	Negative
16	Undecanol	$C_{11}H_{24}O$	Alcohol	1.09	172.64	Negative

Table S9. Results from the study on the α-amylase inhibitory activity and the concentration of IC_{50} value of *C. grandis*

Concentration (in µg/mL)	Acarbose	C. grandis
125	56.39±2.42	70.80±1.16
62.5	53.32±3.42	52.61±0.67
31.25	42.69±3.18	46.3±1.98
15.62	33.69±1.78	43.06±1.1
7.81	26.66±2.5	30.26±0.76
Inhibitory Concentration (IC_{50}) in µg/mL	79.92±8.08	52.40±2.68

Note: All the values are expressed in means of the triplicate